University of Massachusetts Amherst

ScholarWorks@UMass Amherst

Doctoral Dissertations 1896 - February 2014

1-1-1986

Real-time attentional models for classical conditioning and the hippocampus.

Nestor A. Schmajuk
University of Massachusetts Amherst

Follow this and additional works at: https://scholarworks.umass.edu/dissertations_1

REAL-TIME ATTENTIONAL MODELS

FOR CLASSICAL CONDITIONING

AND THE HIPPOCAMPUS

A Dissertation Presented

by

Nestor A. Schmajuk

Submitted to the Graduate School of the
University of Massachusetts in partial fulfillment
of the requirements for the degree of

DOCTOR OF PHILOSOPHY

May 1986

Psychology

REAL-TIME ATTENTIONAL MODELS

FOR CLASSICAL CONDITIONING

AND THE HIPPOCAMPUS
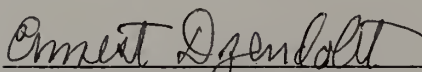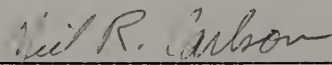
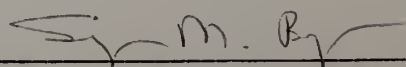A Dissertation Presented

By

Nestor A. Schmajuk

Approved as to style and content by:

John W. Moore, Chairperson of Committee

Andrew G. Barto, Member

Ernest Dzendolet, Member

Neil Carlson, Member

Seymour M. Berger, Department Head
Psychology

ACKNOWLEDGMENT

ABSTRACT

REAL-TIME ATTENTIONAL MODELS
FOR CLASSICAL CONDITIONING
AND THE HIPPOCAMPUS

May 1986

Nestor A. Schmajuk, E.E., University of Buenos Aires

M.A., State University of New York at Binghamton

Ph.D., University of Massachusetts

Directed by : Professor John W. Moore

Schmajuk and Moore (1985) described two real-time
attentional models for classical conditioning. By
assuming that hippocampal lesions (HL) affect computations
that control the rate of learning, both models are able to
simulate HL effects on many classical conditioning
paradigms. The present study introduces two real-time
attentional-associative models that, unlike their
predecesors, allow sensory preconditioning and higher-
order conditioning. In addition, they incorporate
performance rules that convert learning variables into
instantaneous amplitude of the rabbit nictitating membrane
(NM) response and associated neural firing. Computer
simulations using both models were carried out for the
following protocols: acquisition under simultaneous,
delay, and trace conditioning, conditioned inhibition,

extinction, latent inhibition, blocking, mutual overshadowing, sensory preconditioning, discrimination reversal, and hippocampal stimulation and recording during conditioning. Simulated rate of learning, asymptotic level of responding, NM response topography, and hippocampal single unit activity were compared with data obtained with the rabbit NM preparation. Although some discrepancies between simulation results and relevant literature were noted, both models proved capable of simulating a large portion of the experimental data.

TABLE OF CONTENTS

LIST OF TABLES

LIST OF FIGURES

C H A P T E R   I

INTRODUCTION

Background

Over the past thirty years many theories have been
advanced to define the function of the hippocampus in
learning. It has been proposed that the hippocampus is
involved in attention, chunking, contextual retrieval of
information from memory, internal inhibition, long-term
memory selection, recognition memory, response inhibition,
spatial memory, and working memory (See Schmajuk, 1984a,
for a review). Evidence in support of these various
hypothesis has been taken primarily from lesion studies.

Attentional theories emphasize that the hippocampus
is involved in the control of stimulus input. In 1959,
Grastyan, Lissak, Madarasz, and Donhoffer suggested that
the hippocampus inhibits the orienting response to
nonsignificant conditioned stimuli (CSs). Douglas and
Pribram (1966) proposed that the hippocampus excludes from
attention CSs that have been associated with
nonreinforcement. Kimble (1968) proposed that the
hippocampus enables the organism to uncouple its attention
from one stimulus and shift it to new and more
consequential environmental events. Douglas (1972) built

1

on this idea and suggested that the hippocampus is involved in correlating a CS with nonreinforcement, thereby reducing its attentional priority. A closely related hypothesis introduced by Solomon and Moore (1975) is that the hippocampus participates in "tuning out" CSs poorly associated with reinforcement. Moore (1979) proposed a neuronal model to explain how the hippocampus might participate in "tuning out" CSs during conditioning of the rabbit's nictitating membrane (NM) response.

Because most theories of hippocampal function do not specify the nature of interactions between attention and associations, they do not permit unequivocal predictions of the effects of hippocampal lesions (HL) in many conditioning paradigms. The actual meaning of attention in classical conditioning depends on the particular model in which it is defined. Therefore, precise understanding of how attentional variables affect conditioning requires a formal framework in which they are incorporated. Formal models ought to be able to describe normal behavior in tasks sensitive to hippocampal dysfunction, and with changes in attentional variables they also ought to be able to describe the consequences of hippocampal lesions (HL).

The following sections present two formal models that describe normal learning behavior and learning after HL.

Both models are discrete-time models which generate values
of the relevant descriptive variables at discrete time
instants which we denote t = 1, 2, 3,... For convenience
we assume that the basic time step is one abstract unit,
which can be related to various intervals of real time as
required. Both models are expressed as difference
equations specifying how variables change with time. If V
is the variable in question, taking value V (t) at time t,
then we specify its value at time t + 1 by adding $\triangle$ V to V
(t), i.e., V (t+1) = V (t) + $\triangle$ V.

The M-S model.

Moore and Stickney (M-S) (1980) proposed a
mathematical model of hippocampal function in classical
conditioning that meets the above requirements. The M-S
model is based on Mackintosh's (1975) attentional theory
of conditioning. Mackintosh's theory can be represented
by an equation describing the variation of the associative
value (V) between CS_A and the unconditioned stimulus (US)
$\triangle V_A = \propto_A$ k $(\lambda - V_A)$, where k is a constant ($0 < k \leqslant 1$),
$\propto_A$ is the attentional factor representing the CS's
associability ($0 < \propto_A \leqslant 1$), and λ is the asymptote of V_A.
V_A can be interpreted as the prediction of the US by CS_A .
According to Mackintosh (1975), $\propto$ for a given stimulus
increases whenever the outcome of a trial is predicted

better by that stimulus than by any other stimuli on that trial. Otherwise, α decreases.

Moore and Stickney (1980) gave precise quantitative expressions to Mackintosh's rules for changing α : Whenever the outcome of a trial is predicted better by a stimulus, A, than by any other stimulus present with A, α_A increases by $\Delta\alpha_A = c \ (\ 1 - \alpha_A) \ (V_A - V_X)$, where V_A is the associative value of stimulus A and V_X is the the second highest associative value from the set of stimuli presented with A. Otherwise, α_A decreases by $\Delta\alpha_A = c$ $(\ 0 - \alpha_A) \ (V_X - V_A)$, where V_X is the highest associative value from the set of stimuli presented with A. In the M-S model, quantitative rules for computing α depend not only on the associative value between CSs and the US, but also on the associative relationships among the CSs and other events that occur in the learning context.

An additional difference between the M-S and Mackintosh models is that, whereas the Mackintosh model is applicable on a trial-to-trial basis, the M-S model is a real-time model, i.e., it can be applied to the instantaneous values of each learning variable. In the M-S model the variation of the associative value V_A is given by : $\Delta V_A = k \alpha_A \tau_A (1 - V_A)$, where τ_A is the time-varying trace of CS_A. Introduction of trace allows the M-S model to describe the effect that changes in interstimulus

intervals have on change of associative value.

In a refinement of their original model, Moore and Stickney (1982, 1985) introduced a concept not present in the original model, namely the idea of antiassociation. An antiassociation is the prediction of the absence of the US by a CS. The variation of the antiassociative value (N) between CS_A and the US is given by : $\Delta N_A = k \propto_A \overline{C}_A$ $(1 - N_A)$, where k is a constant ($0 < k \leqslant 1$), $\propto_A$ is the attentional factor representing the CS's associability ($0 < \propto_A \leqslant 1$), and $\overline{C}_A$ is the trace of CS_A . The net associative value of a CS with respect to another event such as the US is given by the difference between associative and antiassociative values. The introduction of the concept of antiassociation allows the M-S model to encompass phenomena involving inhibitory conditioning.

In the M-S model salient events include CSs and USs. Each event forms predictive relationships (associations) with all other elements including the context. An event can also form a predictive relationship with itself. Moore and Stickney (1980) referred to the matrix of predictive relationships and corresponding set of associability values, $\propto$, as an attentional-associational network. Associative values are modified under the control of attentional variables computed upon the relationships among the associative values. In the M-S

model, the value of the predictive relation "A predicts B"
is not the same as "B predicts A".

In applying their model to hippocampal function,
Moore and Stickney (1980) proposed that HL prevents
associability from decreasing when it otherwise would. In
this formal sense, therefore, HL prevents irrelevant CSs
from being "tuned out." Simulation studies (Moore and
Stickney, 1980, 1982) show that the model describes the
behavior of animals with hippocampal lesions in latent
inhibition, blocking, and spatial learning. Recent
studies of a revised version of the M-S model (Schmajuk &
Moore, 1986) showed that the model can also describe the
behavior of HL animals in delay and trace conditioning,
conditioned inhibition, extinction, and overshadowing.

The S-P-H model.

Schmajuk (1984b) proposed an alternative approach to
hippocampal function in classical conditioning. This
approach is based on Pearce and Hall's (P-H) (1980) model
of Pavlovian conditioning. In the original P-H model
changes in associative values depend on US intensity.
When the intensity of the US exceeds the intensity
predicted by all CSs acting on a given trial, the
excitatory associative value (V) between CS_A and the US
is increased by: $\Delta V_A = S_A \propto_A \lambda$, where S_A is proportional

to the stimulus salience ($0 < S_A \leqslant 1$), α_A is the associability ($0 < \alpha_A \leqslant 1$), and λ the US intensity. When the intensity of the US predicted by all CSs acting on a given trial exceeds the actual intensity of the US, the inhibitory associative value (N) between CS_A and the US is increased by: $\Delta N_A = S_A \alpha_A \bar{\lambda}$, where $\bar{\lambda}$ is the difference between the predicted intensity of the US and the actual intensity. As in the M-S model, the net associative value is given by the difference between excitatory and inhibitory associative values.

Associability of a given CS in the P-H model depends on the predictions of the US made by all the CSs acting on the previous trial and on the associability of CS on previous occasions: $\alpha_A^n = \gamma \mid \lambda^{n-1} - \sum V^{n-1} \mid + (1 - \gamma) \alpha_A^{n-1}$, where n refers to the present trial, n - 1 refers to the preceding trial, γ is a parameter ($0 < \gamma \leqslant 1$), $\sum V^{n-1}$ is the sum of the associative values of all CSs present on the preceding trial, λ^{n-1} is the US intensity on the previous trial, and α^{n-1} is the associability on the previous trial. Unlike the Mackintosh and M-S models, where the associability of a given CS increases as its association with the US increases, in the P-H model associability of a given CS decreases as its association with the US increases. In order to describe the effects of HL in terms of the P-H model, Schmajuk (1984b) proposed

that HL causes the associability of a CS on trial n to be independent of its previous values and of predictions of the US made by other CSs.

In order to circumvent certain problems of the P-H model in partial reinforcement paradigms (Pearce, Kaye, and Hall, 1982), Schmajuk and Moore (1986) introduced modifications in the original model. A model that incorporates real-time expressions for the equations defining associative and attentional variables, was designated the S-P-H model. Computer simulations of a revised version of the S-P-H model (Schmajuk & Moore, 1986) show that with the assumptions regarding HL proposed by Schmajuk (1984b) the model describes the behavior of HL animals in delay conditioning, partial reinforcement, differential conditioning, extinction, latent inhibition, blocking, overshadowing, and discrimination reversal.

Goals of the present study

In their present forms, both the M-S and the S-P-H models are capable of real-time descriptions of the behavior of normal and HL animals in many classical conditioning paradigms. However, these models do not encompass either higher-order conditioning or sensory preconditioning.

Furthermore, the M-S and the S-P-H models do not provide explicit performance rules that permit real time descriptions of conditioned response topography. Since performance rules mapping learning variables into behavioral variables are peculiar to each experimental situation, a preparation must be selected. The large amount of data on classical conditioning of the rabbit NM makes this preparation particularly attractive for a formal treatment. In addition, the effect of HL on NM classical conditioning has been extensively described (e.g., Solomon and Moore, 1975), single unit activity of the hippocampus during the rabbit's NM classical conditioning has been carefully analyzed (Berger, Rinaldi, Weisz, and Thompson, 1983), and the effect of electrical hippocampal stimulation (HS) has been reported (Berger, 1984; Prokasy, Kesner, and Calder, 1982).

Therefore, the present study contrasts experimental results regarding the hippocampal formation in the NM preparation with computer simulations using two attentional-associative models built with M-S or S-P-H elements. Relevant data include HL and HS experiments and hippocampal recording studies.

ATTENTIONAL-ASSOCIATIVE MODELS

This section describes a class of attentional-associative models that can be applied to CS-CS paradigms, such as sensory preconditioning and higher-order conditioning, as well as CS-US paradigms.

Consider the case of one CS, CS_i , that predicts event k. Associative value, V_i^k , represents the prediction of event k by CS_i . Antiassociative value, N_i^k, represents the prediction of the absence of event k by CS_i.

Net prediction of event k by CS_i is represented by the net associative value, $\dot{V}_i^k$, and is given by $V_i^k - N_i^k$.

Consider now the case of two CSs, CS_i and CS_r, that predict event k. $\dot{V}_i^k$ is the first-order net prediction of event k by CS_i , and $\dot{V}_r^k$ is the first-order net prediction of event k by CS_r . It is assumed that CS_i predicts event k directly by $\dot{V}_i^k$ and indirectly by predicting CS_r , by $\dot{V}_i^r$. In turn, CS_r predicts event k by $\dot{V}_r^k$. The second-order net prediction of event k by CS_i , is expressed as the product $\dot{V}_i^r \dot{V}_r^k$. The second-order net prediction of event k by CS_i is one when $\dot{V}_i^r$ and $\dot{V}_r^k$ are both one, and zero when either $\dot{V}_i^r$ or $\dot{V}_r^k$ is zero.

B_i^k , the sum of first- and second- order predictions of event k by CS_i , is

$$B_{i}^{K} = (\ \dot{V}_{i}^{K}\ +\ \sum_{r} w_{i}^{r}\ \dot{V}_{i}^{r}\ \dot{V}_{r}^{K}\ )\ \tau_{i}\ . \qquad [1]$$

$\dot{V}_{i}^{K}$ is the net associative value of CS_{i} with event k. The sum over index r involves all the CSs with index $r \neq k$. $\dot{V}_{i}^{r}$ is the net associative value of CS_{i} with all CSs with index $r \neq k$. $\dot{V}_{r}^{K}$ is the net associative value of all CS_{r} with event k. τ_{i} is the trace of CS_{i}. The mathematical expression for τ_{i} is given below. Coefficient w_{i}^{r} serves to adjust the relative weights of first- and second-order predictions in paradigms such as conditioned inhibition. In order to avoid redundant CS_{i} - US and CS_{i} - CS_{i} - US associations, $w_{i}^{r} = 0$ when i = r, and w > 0 when $i \neq r$.

B^{K}, the aggregate prediction of event k made upon all CSs (including the context) with $\tau_{i} > 0$ at a given moment, is given by

$$B^{K} = \sum_{i} B_{i}^{K}\ . \qquad [2]$$

The sum over index i involves all the CSs acting at a given moment.

Variable B^{K} participates in the rules governing the computation of V, N, and $\propto$ in the models. In addition, B^{US} determines the topography of the NM response, as described below.

The M-S-S model

The preceding section described a basic structure for models that can be applied to CS-CS and CS-US associations. This section describes an attentional-associative model that incorporates the variable B and includes refinements introduced by Schmajuk and Moore (1986) that correct deficiencies in earlier versions of the M-S model in describing extinction, partial reinforcement, and reacquisition following extinction. The model introduced in this section has been designated the M-S-S model.

Changes in associative values.

When CS_i is accompanied or followed by event k, the associative value between CS_i and k, V_i^K, increases by

$$\Delta V_i^K = \theta \alpha_i \sigma_i \ (1 - V_i^K). \qquad [\ 3\ ]$$

The antiassociative value, N_i^K, decreases by

$$\Delta N_i^K = \theta \alpha_i \sigma_i \ (0 - N_i^K). \qquad [\ 3'\ ]$$

When event k does not occur, V_i^K decreases by

$$\Delta V_i^K = \theta' \alpha_i \overline{\sigma}_i \; (\; 0 - V_i^K \;) \; B^K \;, \; [\; 4 \;]$$

and N_i^K increases by

$$\Delta N_i^K = \theta' \alpha_i \overline{\sigma}_i \; (\; 1 - N_i^K \;) \; B^K \;, \; [\; 4' \;]$$

where α_i is CS_i's associability, θ ($0 < \theta \leqslant 1$) is the rate of change in V_i^K and N_i^K when event K is present, θ', $0 < \theta' < \theta$, is the rate of change in N_i^K and V_i^K when event k is absent, $\overline{\sigma}_i$ is the trace of CS_i , and B^K is defined by Equation 2.

It should be noted that λ in the Mackintosh's model has been replaced by 1 or 0 in Equations 3 and 4. V_i^K and N_i^K are interpreted as the degree of "belief" that CS_i is or is not followed by event k, and this belief is placed on a scale 0 to 1. Events differing only in their intensities, implying different λ in Mackintosh's (1975) model, are treated as different events in the M-S and M-S-S models.

The net associative value of CS and event k is given by the difference between associative and antiassociative values

$$\dot{V}_i^K = V_i^K - N_i^K \; .\qquad\qquad [\; 5 \;]$$

Net first-order predictions given by Equation 5 are used in Equation 1. When i = k, V_i^i defines the net prediction of the event i by itself. The magnitude of V_i^i increases with increasing CS duration and increasing number of trials.

Changes in associability.

The associability of CS_i, α_i, may increase, decrease, or remain unchanged depending on the associative value of CS_i with event k and the associative value of another stimulus, CS_j, with event k.

When CS_i, CS_j, and event k are presented together, and provided that $\dot{V}_i^K > \dot{V}_j^K$

$$\Delta \alpha_i^K = c \, (\, 1 - \alpha_i^K) \, (\dot{V}_i^K - \dot{V}_j^K), \qquad [\ 6\ ]$$

where $\dot{V}_j^K$ is the second highest associative value with respect to event k of all the stimuli present with CS_i, including the context.

When $\dot{V}_j^K >= \dot{V}_i^K$

$$\Delta \alpha_i^K = c \, (\, 0 - \alpha_i^K) \, (\dot{V}_j^K - \dot{V}_i^K), \qquad [\ 7\ ]$$

where $\dot{V}_j^K$ is the highest associative value with respect to k of all the CSs present with CS_i. Parameter c in

Equations 6 and 7 is a constant set $0 < c \leqslant 1$.

As in the original M-S model, the components of $\Delta\alpha_i$ relating CS_i to event k are combined in the expression

$$\Delta\alpha_i = \sum_K \phi_K \Delta\alpha_i^K / \sum_h \phi_h \qquad . \qquad [\ 8\ ]$$

The sum over the index k in the numerator involves all the target events present with CS_i . The sum over the index h in the denominator involves all the events encountered by the subject in previous experiences in the same context, even though they may not be present at the time $\Delta\alpha_i$ is computed. The weighting factors, ϕ_K , are selected such that $\phi_{US} > \phi_{CS} > \phi_X$, because the US is presumed to be biologically more significant than CSs or the context (X).

Effects of hippocampal lesions and hippocampal stimulation.

As mentioned before, Moore and Stickney (1980) assigned to the hippocampus the task of decreasing α . Thus, HL renders all the expressions of the form of Equation 7 equal to zero. All other computations proceed normally.

Regarding HS, it is assumed that CS_i 's associability increases when HS is applied. In the absence of HS all computations proceed normally.

The S-P-H model

The preceding section described a model in which net associative values, $\overset{\bullet}{V}{}_i^K$, and associability, α_i, are computed with revised M-S elements. In this section we describe a model in which $\overset{\bullet}{V}{}_i^K$ is computed with S-P-H rules.

In the original P-H model superscripts were used to denote trial number. In the present version of the model subscripts are used to denote CSs, superscripts are used to specify target events, and α and λ are values for the current time step t.

It should be noted that, whereas in the M-S model λ is equal to either 1 or 0, in the S-P-H model it has a continuous value. Therefore, unlike the M-S-S model, two target events differing only in their intensities are not regarded as different events. In the S-P-H model intensity of event k is represented by λ^K.

Changes in associative values.

Whenever the intensity of event k, λ^K, is greater than B^K as defined by Equation 2, the excitatory associative value between CS_i and event k, $\overset{\bullet}{V}{}_i^K$, increases by

$$\Delta V_i^K = \theta \; s_i \; \alpha_i^K \; \lambda^K \; \sigma_i \; , \qquad\qquad [\; 9\;]$$

where θ is the rate of change of V_i^K , S_i is the salience of CS_i, α_i^K represents the associability of CS_i with event k, λ^K represents the intensity of event k, and $\overline{\sigma}_i$ represents the trace of CS_i .

Whenever $\lambda^K \leqslant B^K$, the inhibitory associative value between CS_i and event k, N_i^K, increases by

$$\Delta N_i^K = \theta' \ S_i \ \alpha_i^K \overline{\lambda}^K \overline{\sigma}_i,$$ [10]

where θ' is the rate of change of N_i^K , and $\overline{\lambda}^K = B^K - \lambda^K$.

The net associative value of a CS_i with event k is

$$\dot{V}_i^K = V_i^K - N_i^K$$ [11]

When i = k, $\dot{V}_i^i$ defines the net prediction of the event i by itself. The magnitude of $\dot{V}_i^i$ increases with increasing CS duration and increasing number of trials. Net first-order predictions given by Equation 11 are used in Equation 1 to compute B_i^K .

Changes in associability.

The associability of CS_i with event k at time step t

is given by

$$\alpha_i^\kappa (t) = \; | \; \lambda^\kappa (t) - B^\kappa (t) \; |$$ [12]

It should be noted here that, by Equation 9, V_i^κ does not increase when α_i^κ is zero. As defined by Equation 12, is zero when B^κ equals λ^κ. Therefore, Equation 12 ensures that B^κ will not exceed λ^κ.

An alternative expression for computing α_i^κ, is

$$\alpha_i^\kappa (t) = \gamma \; | \; \lambda^\kappa (t) - B^\kappa (t) | + (1 - \gamma) \; \alpha_i^\kappa (t - 1)$$ [12']

Equation 12' computes α_i^κ as a weighted average of the absolute difference between λ^κ and B^κ and the α s for previous time steps. Whereas Equation 12 depends on the instantaneous values of B^κ and λ^κ, Equation 12' implies a memory for the past values of α.

When defined by Equation 12', α_i^κ might be greater than zero even when B^κ equals λ^κ. Therefore, use of Equation 12' without further restrictions allows B^κ to exceed λ^κ. In order to avoid this overprediction, whenever event k is present, use of Equation 12' is restricted to those cases in which $\alpha_i^\kappa (t - 1)$ is smaller than $| \lambda^\kappa (t) - B^\kappa (t) |$. When $\alpha_i^\kappa (t - 1)$ is greater than $| \lambda^\kappa (t) - B^\kappa (t) |$, Equation 12' is used with $\gamma = 1$. This

procedure ensures that B^K has an upper limit equal to λ^K.

Changes in salience.

In both the P-H and S-P-H models, salience S_i is a constant. However, in the present model rendering of the S-P-H model, S_i is defined by

$$S_i = \delta_i + \alpha_i^i \qquad [\ 13\ ]$$

where δ_i is a constant and α_i^i is the associability of CS_i with itself.

Replacing α_i^i by its value in Equation 12, it results

$$S_i = \delta_i + \mid \lambda^i - B^i \mid \qquad [\ 13'\ ]$$

Equation 13 implies that when α_i^i equals zero salience S_i equals δ_i. According to Equation 13', α_i^i equals zero when the intensity of CS_i is perfectly predicted by all acting CSs including itself at a given time step. Conceptually, this means that salience S_i decreases as CS_i becomes increasingly "familiar" to the animal. Larger increments in V^K and N_i^K are obtained with novel rather than with familiar CSs.

In addition, Equation 13 implies that when CS_i is predicted by a CS preceding it, CS_r , the association

between CS_r and CS_i retards the formation of the association between CS_i and event k. This property is used below to describe succesive conditional responding.

Equation 13 is also used to yield latent inhibition, i.e., the effect of CS preexposure in the absence of the US on the subsequent acquisition of the CS-US association. Wagner (1979) proposed a similar mechanism for latent inhibition in the context of the Rescorla-Wagner (1972) model. In the original and revised versions of the P-H model, S_i is assumed to be a constant, and latent inhibition is predicted by the use of an equation similar to Equation 13': CS_i preexposure in the absence of the US reduces the value of α_i^i, thereby retarding subsequent acquisition of the CS-US association.

Effect of hippocampal lesions and hippocampal stimulation.

It is assumed that in the case of HL, depends not on B^K, but on B_i^K. In addition, the model assumes a deficit in the computation of CS-CS associations, and therefore all $\dot{V}_i^r$ equal zero. As a consequence, associability is given by

$$\alpha_i^K = |\lambda^K - \dot{V}_i^K|, \qquad [\ 14\ ]$$

and $\bar{\lambda}$ by

$$\bar{\lambda} = \dot{v}_i^{\kappa} - \lambda^{\kappa} \quad , \qquad\qquad [\ 15\ ]$$

Equations 14 and 15 imply that the upper limit for $\dot{v}_i^{\kappa}$ is
the intensity of event k.

After HL, salience S_i is given by

$$S_i = \delta_i + \lambda^i \quad , \qquad\qquad [\ 16\ ]$$

Equation 16 implies that salience does not decrease over
trials, or equivalently, that the CS does not become
increasingly "familiar" in time. Use of Equation 16
implies impairments in latent inhibition. .

Because all $\dot{v}_i^r$ equal zero, B_i^{κ} , defined in Equation
1, is given by

$$B_i^{\kappa} = \dot{V}_i^{\kappa} \quad . \qquad\qquad [\ 17\ ]$$

The effects of HS are described by applying Equation
12'. It is assumed that HS prior to conditioning trials
enhances the value of α (t - 1), thereby increasing α on
subsequent time steps.

C H A P T E R   III

NM RESPONSE CONDITIONING

The rabbit's NM response has been used extensively as
a model system to study classical conditioning (see
Gormezano, Kehoe, & Marshall, 1983). In the NM response
preparation the nictitating membrane (NM) extension is
measured by a displacement transducer whose signal is
amplified and recorded. The CS is typically a tone or a
light, and the US is either a puff of air delivered to the
dorsal region of the cornea, or electrostimulation
administered to the periocular region. In these
conditions, acquisition of the conditioned response (CR)
proceeds with an orderly sequence of changes: Percentage
of NM responses generated in each session increases, CR
latency decreases, and CR amplitude increases. This
sequence is reversed in extinction.

The CR latency moves progressively forward in the CS-
US interval with training (Smith, 1968). At the beginning
of training CR the first CRs are initiated just before the
unconditioned response (UR), but initiation moves to
progressively earlier portions of the CS-US interval with
an asymptotic latency occurring at about the midpoint of
the CS-US interstimulus interval (ISI). As CR onset
latency decreases the maximal response amplitude (CR peak)

tends to be located around the time of the US ocurrence.
Systematic manipulations of the ISI affects CR topography.
At ISIs of zero CRs are negligible, at ISIs of around 200
msec CRs increase dramatically, and for longer ISIs CRs
gradually decrease (Schneiderman, 1966; Smith, 1968).

The trace hypothesis

Conditioning of the NM is typically more efficacious
when the CS precedes the US than when the two are
presented together (Gormezano et al., 1983). Theorists
have proposed that stimuli give rise to traces in the
central nervous system that somehow impinge simultaneously
on critical loci of learning, despite the non-simultaneous
arrangement as obseved at the periphery. Hull (1943), for
example, proposed that CS onset initiates a trace which
increases over time to a maximum and then gradually decays
back to zero. The increment in the associative value on
each trial is a function of the intensity of the trace at
the time the US is presented. Thus, the curve
representing CR strength as a function of the
interstimulus interval (ISI) presumably reflects the
variation in trace intensity over time (Gormezano et al.,
1983). This scheme allows learning consistent with
contiguity principles.

Gormezano (1972) proposed that the decrease in CR latency with increasing number of trials results from generalization of the trace intensity at the time of the US presentation to the intensity of earlier portions of the trace. The generalization hypothesis correctly predicts that if the US is presented at or before the time that the trace reaches its maximum the first CRs occur just before the US. Subsequently, CR latency decreases progressively towards CS onset because of generalization. However, the hypothesis encounters difficulties if the US occurs after the trace reaches its maximum: For any point in the decaying part of the trace, there is also one point in the raising part of the trace that has the same amplitude. If the amplitude of the point of the decaying part of the trace is associated to the US, the hypothesis predicts that a CR occurs at a point of the raising part of the the trace, i.e., before it actually appears. Therefore, an alternative mechanism to Gormezano's trace generalization hypothesis is needed in order to account for changes in CR latency.

In the present paper, it is assumed that a CS_i generates a trace, σ_i. This trace increases over time to a maximum, stays at this level for a period of time independent of CS duration, and then gradually decays back to zero.

Formally, and specifically for the rabbit NM preparation, the trace is defined for t <= 200 msec by

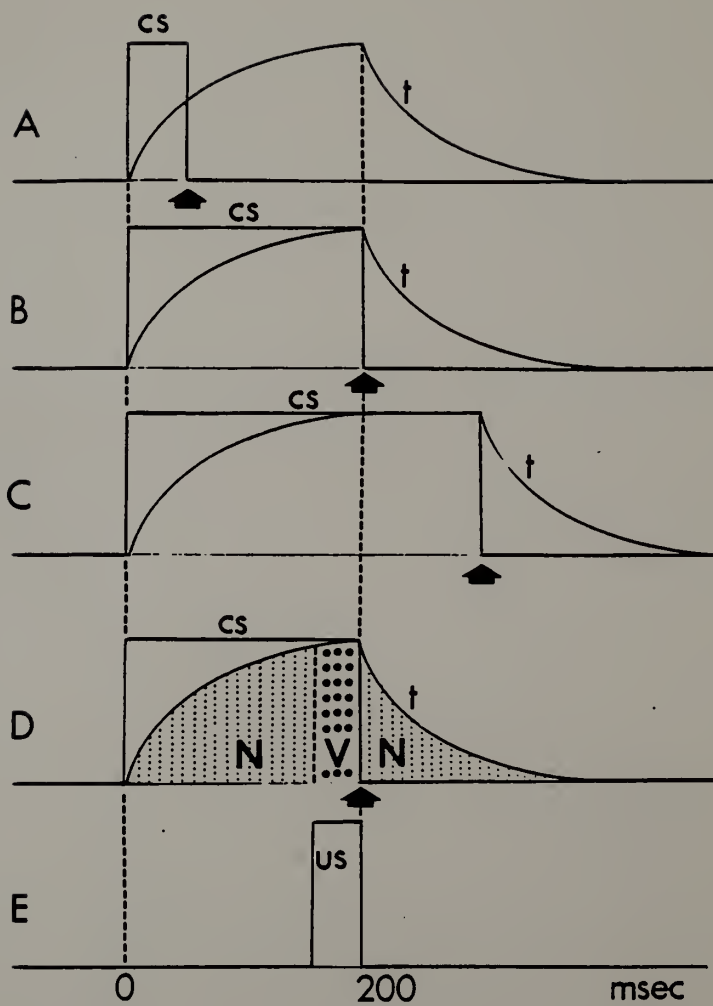$$\vec{\sigma}_i(t) = CS_i\, max\,(\,1 - exp\,[\,-k1\,t\,]\,), \qquad [\,18\,]$$

where CS_i max is the maximum intensity of the trace recruited by CS_i from its onset to its offset, and k1 is a constant, $0 < k1 \leqslant 1$. Parameter k1 is selected so that, when applying Equations 3, 4, 9, and 10, the ISI for NM optimal conditioning is 200 msec. By Equation 18, for any CS duration the amplitude of the trace rises during the first 200 msec after CS onset. $\vec{\sigma}_i(t)$ remains equal to CS_i max as long as CS_i does not decay. If $CS_i = 0$ and t > 200 msec, $\vec{\sigma}_i(t)$ decays by
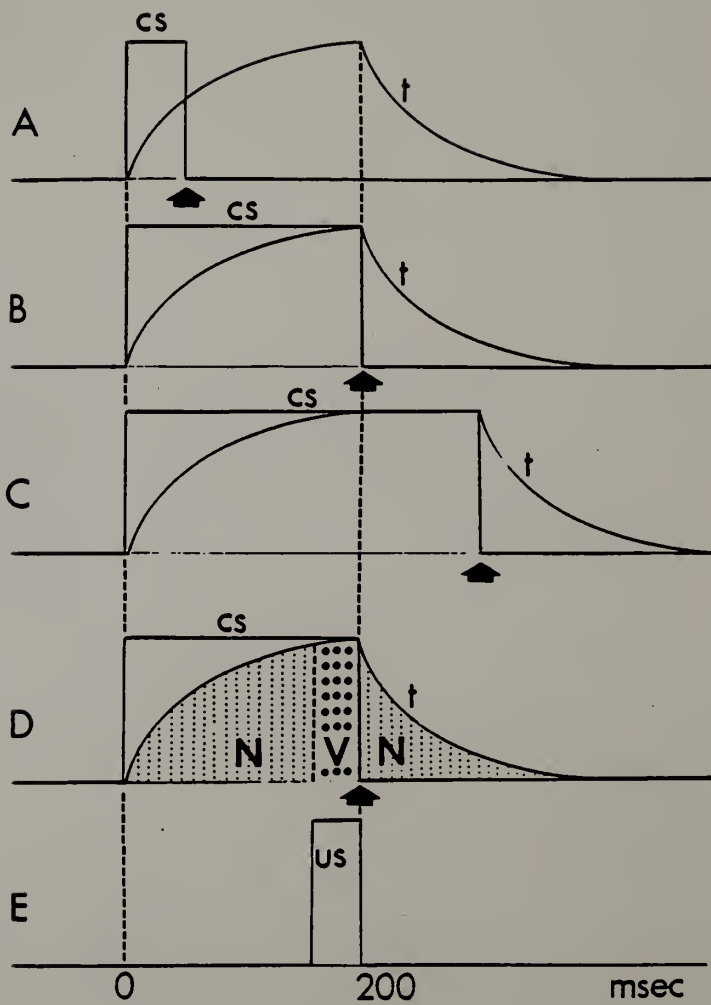
$$\vec{\sigma}_i(t) = CS_i\, max\,(\,exp\,[\,-k1\,t\,]\,), \qquad [\,19\,]$$

If CS_i is not present 200 msec after its onset, the trace decays to zero by Equation 19.

Figure 1 illustrates how Equations 18 and 19 are applied. Panels A, B, and C show the trace for CSs of 50-msec, 200-msec, and 300-msec duration. For a CS shorter than or equal to 200 msec the trace grows for 200 msec before decaying to baseline. For a CS longer than 200

msec the trace remains at maximum strength as long as the CS is present, after which it decays to baseline. Panel D shows how the trace is associated with either the presence or the absence of the US. As it will be discussed below, rules governing associations between the trace and the presence or the absence of the US vary according to the model that is applied to the computation of V and N.

Performance Rules

Performance rules were selected to relate variable B to the topography of the NM response. Performance rules allow the computation of the instantaneous values of CR using the instantaneous values of B^{US}.

The NM response is characterized by (a) the latency to CR onset, (b) shape during the CS period, (c) shape during the US period, and (d) decay to baseline.

Latency to CR onset.

Let t_{CS} denote the time step at which CS onset occurs. Then the time of CR onset, denoted t_{CR} , is the earliest time t such that

$$\sum_{t'=t_{CS}}^{t} \sum_{j} B_{j}^{US}(t') \; >= \; L1. \qquad [\ 20\ ]$$

The sum over the index j involves B_j^{US} of all CSs with $\zeta_j >$ 0, excluding the context. The sum over index k involves all time steps or which $\zeta_j > 0$, starting at the time step when the amplitude of the NM response as defined by Equations 21 and 22 equals zero (see below). Time increments, Δt, are equal to one time step. L1 is a threshold greater than zero. Equation 20 implies that as B_j^{US} increases over trials, CR onset latency moves progressively toward an asymptote determined by L1.

CS period.

For time steps $t > t_{CR}$, i.e., after the time of the CR onset, the amplitude of the NM response, NMR (t), is changed by

$$\Delta NMR\ (t) = k2\ (\ B^{US}(t)\ -\ NMR\ (t)).\qquad [\ 21\ ]$$

where k2 is a constant $(0 < k2 \leqslant 1$). By Equation 1, B^{US} (t) increases with the time constant k1 of trace ζ_i , k2 is selected k2 > k1 so that NMR (t) reaches B^{US}(t) during the CS period. For $t < t_{CR}$, the amplitude does not change.

US period.

During the US period, while B^{US} (t) $> \lambda^{US}$(t), NMR (t)

still increases by Equation 21. However, when $\lambda^{US}(t) > B^{US}(t)$, NMR (t) increases by

$$\triangle NMR\ (t) = k2\ \ (\lambda^{US}(t) - NMR\ (t)) \qquad [\ 22\ ]$$

Decay to baseline.

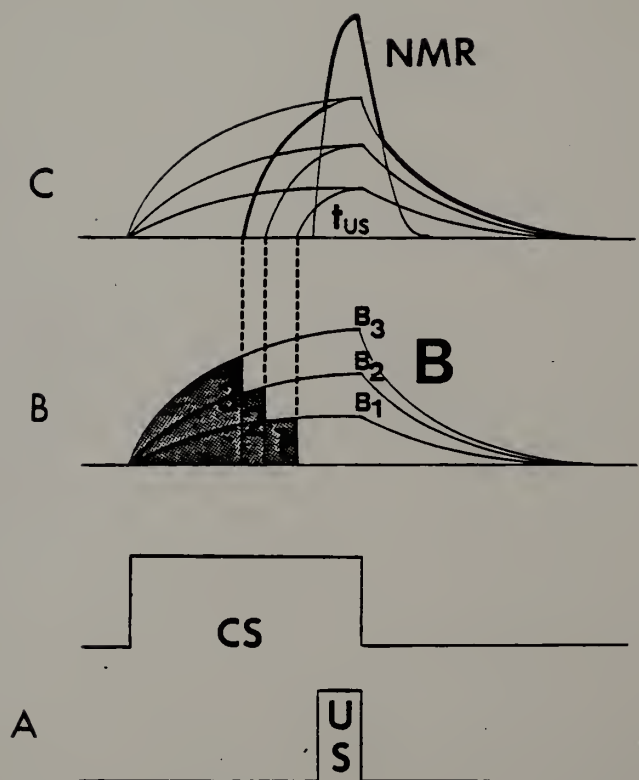When $B^{US}(t)$ and $\lambda^{US}(t)$ equal zero, NMR (t) decays to baseline by

$$\triangle NMR\ (t) = -\ k2\ NMR\ (t) \qquad [\ 23\ ]$$

By Equations 21, 22, and 23, NMR (t) is bounded between zero and one in the case of the M-S-S model, and zero and in the case of the S-P-H model.

Figure 2 illustrates how the NM response topography is generated. B 1 , B 2 , and B 3 represent different values of B^{US} . These different values of B^{US} may have arise from an increasing number of pairings with the US, association with another CS associated with the US, or by way of training with various ISIs. In Fig. 2 areas 1, 2, and 3 are equal to threshold L1 at times 1, 2, and 3 respectively. During the CS period NMR (t) approaches B 1 , B 2 , or B 3 , respectively, by Equation 21. During the US period NMR (t) approaches λ^{US}, by Equation 22. In the absence of both CS and US, NMR (t) decays to zero by

Figure 2

NM response topography. Panel A: 200 msec CS and
50 msec US are presented together. Panel B: Equal
Areas 1, 2, and 3 under increasingly higher B(t)
curves are bounded respectively by times t1 > t2 >
t3. Times t1, t2, and t3 indicate CR onsets
corresponding to B1, B2, and B3. Panel C: NMRs are
generated according to Equations 21 and 22 with CR
onsets determined in Panel B.

Equation 23.

C H A P T E R   IV

METHOD

Simulations describing NM topography of normal, HL, and HS animals were carried out with the M-S-S and S-P-H models. This section defines and justifies the values of the different parameters adopted for the simulations.

In the simulations continuous time was converted to discrete time steps or bins, equivalent to 10 msec duration. Each trial consisted of 60 bins, equivalent to 600 msec. Unless specified, the simulations assumed 200 msec CSs, the last 50 msec of which overlaps the US. CS onset was at 200 msec. Parameters were selected so that simulated asymptotic values of V and were reached after 10 acquisition trials. Since asymptotic conditioned NM responding is reached in aproximately 200 trials (Gormezano et al., 1983), one simulated trial is approximately equivalent to 20 experimental trials.

The right upper panel of all figures displaying simulation results shows net associative values at the end of each trial (60 time steps). For simulations with the M-S-S model, the right lower panel shows associabilities at the moment the US is presented on reinforced trials, as a function of trials. For simulations with the S-P-H model, the right lower panel shows the product of

34

associabilities multiplied by salience at the moment the
US is presented on reinforced trials, as a function of
trials. The left panel shows NM response topography as a
function of time and trials.

M-S-S model

For simulations with the M-S-S model, parameter
values for variations of associative values were : θ =
0.1, and θ' = 0.001. In order to obtain positive values
of V, θ was set 100 times greater than θ'. As shown in
Fig.1 (Panel D and E), increments in V during the few time
steps when the US is present need to overcome decrements
in V during the many time steps when the US is absent.
For antiassociative values were : θ = 0.1 and θ' = 0.005,
with exception of the inhibitory conditioning cases, for
which θ' = 0.05. θ was set 20 time greater than θ' in
order to obtain adequately small values of N. As shown in
Fig. 1 (Panel D and E), decrements in N during the few
time steps when the US is present should compensate
increments in N during the many time steps when the US is
absent. Increments in θ allow convergence to the desired
values of N with a reduced number of trials. Initial
values of Vs and Ns were zero. In the extinction
protocols the initial values of Vs, Ns, and αs were made

equal to the final values resulting from the delay
acquisition simulation.

For variations in associability : $\phi_{US} = 1$, $\phi_A = 0.16$, ϕ_B
$= 0.16$, $\phi_X = 0.01$, and c = 0.6, because the US is presumed
to be represented in memory more strongly than the CSs,
and the CSs more strongly than the context. Initial
values of associability were always selected $\alpha_X = 0.1$ and α_A
$= \alpha_B = 0.5$, giving an intermediate value to the newly
presented CSs and a low value to the context, on the
assumption that associabilities are proportional to their
relative saliences.

For computations of B_i^K : $w_i^r = 0.4$ when i = r. The
value of w_i^r was selected so as to allow the model to
display secondary reinforcement before conditioned
inhibition in a secondary reinforcement paradigm. In
order to avoid redundant CS_i -US and CS_i - CS_i -US
associations, w_i^r equals zero when i = r.

S-P-H model

For simulations with the S-P-H model, initial values
of Vs and Ns were zero. In the extinction protocols the
initial values of Vs, Ns, and α s were set equal to the
final values resulting from the delay acquisition
simulation. Parameters values for variations of V and N

were : $\Theta = 0.030$, and $\Theta' = 0.015$. In order to obtain

positive values of $\overset{\cdot K}{V_i}$, Θ was set 2 times greater than Θ'.

As shown in Fig.1 (Panel D and E), increments in V during

the few time steps when the US is present should overcome

increments in N during the many time steps when the US is

absent. In the inhibitory conditioning cases it was $\Theta' = 0.030$. The increased value of Θ allows convergence toward

the desired values of N with a reduced number of trials.

Initial values of associability were always set equal to

zero.

For computations of $\overset{K}{B_i}$: $\overset{r}{w_i} = 2$ when $i \neq r$. The value

of $\overset{r}{w_i}$ was selected so as to allow the model to display

secondary reinforcement before conditioned inhibition in a

secondary reinforcement paradigm. In order to avoid

redundant CS_i -US and CS_i - CS_i -US associations, w_i^r equals

zero when $i = r$. The constant part of S_i , δ_i , was set

equal to 0.5 for every CS.

The S-P-H model assumes that HS enhances the value of

α thereby increasing α on subsequent time steps and

facilitating the acquisition of classical conditioning.

In order to provide a mechanism for storing the enhanced

value of α , simulations of the effect of HS were carried

out using Equation 14' instead of Equation 14. γ in

Equation 14' was set equal to .9.

NM response topography

For computation of σ_L: k1 = 0.1, which is the appropiate value for an optimal ISI of 200 msec. For computations of the NM CR onset: L1 was set equal to 2, in order to have CR onset latencies asymptote at approximately the midpoint of the ISI. For the NM response topography: k2 = 0.5, which ensures that the NM response reaches the value of B^{US} within the CS period.

Neural activity

Hippocampal neural activity was simulated by assuming that hippocampal neurons code the instantaneous magnitude of variables that are used in the computation of α, $\dot{V}_L^{US}$ in the M-S-S model, and B^{US} in the S-P-H model. The magnitude of either variable was translated into neuronal firing by applying the following rules. If at time $t > t_{cs}$, $\sum_{t'=t_{cs}}^{t} f(t') < L2$ no spike is generated. If at time $t > t_{cs}$, $\sum_{t'=t_{cs}}^{t} f(t') > L2$ a spike is generated and the sum is reset to zero. In the M-S-S model $f(t') = \dot{V}_L^{US}$, and in the S-P-H model $f(t') = B^{US}$. The threshold L2 was set equal to .5 , in order to allow neural activity to precede the onset of the NM response.

CHAPTER V

COMPUTER SIMULATIONS

Simulations describing the NM topography of normal
and HL animals were carried out with the M-S-S and S-P-H
models. The following procedures were simulated for the
normal and HL case: simultaneous, delay, and trace
conditioning, conditioned inhibition, extinction, latent
inhibition, blocking, mutual overshadowing, discrimination
reversal, and sensory preconditioning. In addition,
neuronal recordings during acquisition, and acquisition
after hippocampal stimulation, were simulated with both
models for the normal case. This section presents
relevant experimental data and contrasts the data with the
results of the computer simulations.

Acquisition of classical conditioning

Experimental data.

Several studies describe the effect of HL on
acquisition rates. Using a delayed conditioning paradigm,
Schmaltz and Theios (1972) found faster than normal
acquisition of the conditioned nictitating membrane (NM)
response in HL rabbits with a 250-msec CS, a 50-msec US,
and a 250-msec ISI. In contrast with these data, Solomon

and Moore (1975) and Solomon (1977) found no difference in
the rate of acquisition between normal and HL rabbits in
forward delayed conditioning of the NM response using a
450-msec CS, a 50-msec US, and a 450-msec ISI. Port,
Mikhail, and Patterson (1985) examined the effects of HL
on acquisition rates of the NM response in groups of
rabbits trained with 150-, 300-, or 600-msec ISIs. For
all groups CS and US durations were 800 msec and 50 msec,
respectively. Acquisition rates were accelerated and
animals produced more CRs than normals in the 150-and the
600-msec HL groups, but not in the 300-msec HL group.

Several studies describe the effect of HL on NM
topography during acquisition. Solomon and Moore (1975)
and Solomon (1977) found that conditioned response (CR)
topography did not differ in normal and HL rabbits in
forward delayed conditioning of the NM response using a
450-msec CS, a 50-msec US, and a 450-msec ISI. However,
Orr and Berger (1985) found that the area under the NM
response curve was greater for HL animals than for
operated controls in the later phases of a delay
conditioning paradigm using a 850-msec CS, a 100-msec air
puff US, and a 750-msec ISI. Port and Patterson (1984)
found that CR latency was shorter in rabbits with fimbrial
lesions (i.e., hippocampal output) than in rabbits with
cortical or sham lesions, mainly during the first day of

acquisition. Port et al. (1985) examined the effects of
HL on the topography of the NM response in groups of
rabbits trained with an ISI of 150-, 300-, or 600-msec.
Response onset latencies were shorter in the HL group than
in the control groups with the 150-msec ISI, but groups
did not differ with 300- or 600-msec ISIs.

Solomon, Vander Schaaf, Thompson, and Weisz (in
press, 1986) report that CR onset latencies were shorter
in HL rabbits than in normal rabbits trained in a trace
conditioning paradigm using a 250-msec tone CS, a 100-msec
air puff US, and a 750-msec and 2250-msec ISIs. Patterson
(personal communication, 1984) observed similar effects in
HL rabbits trained in a trace conditioning paradigm, when
air puff, but not eye shock, was used as the US. In
summary, CR onset latencies often become shorter, but
sometimes remain unaffected after HL.

Simulation results.

Acquisition of classical conditioning was simulated
with ISIs of 0, 200, and 300 msec. Both CS and US were 50
msec in duration. Figures 3a and 3b show simulations of a
simultaneous conditioning paradigm with the M-S-S and S-P-
H models, respectively. In this paradigm, simulations for
the normal case with both the M-S-S and the S-P-H models
show that CRs occurred late in the trial during the 10

Figure 3a

M-S-S model: Simultaneous conditioning. L: HL
case. N: normal case. A : CS(A). X : Context.
Left Panels: NM response topography in 10
reinforced trials and a test trial. Upper-Right
Panels: Net associative values (VT) at the end of
each trial, as a function of trials. Lower-Right
Panels: Associability (ALPHA) at 200 msec, as a
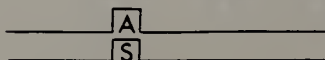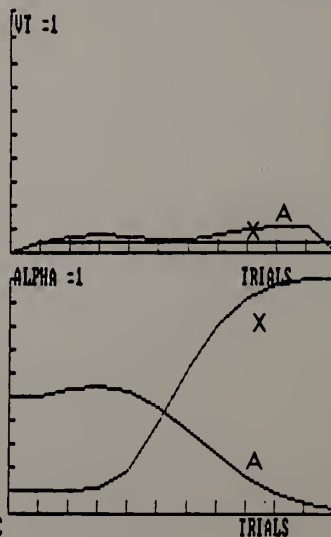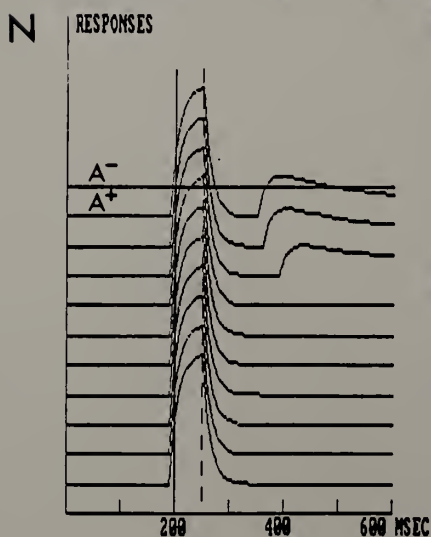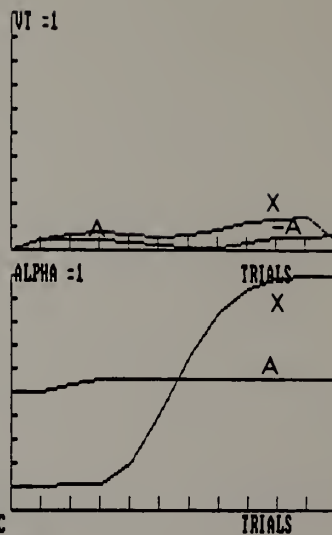function of trials.
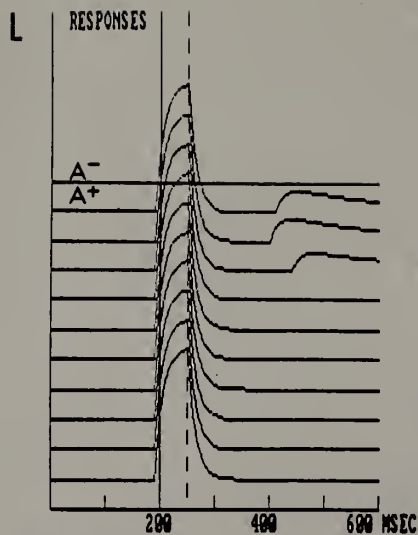
Figure 3b

S-P-H model: Simultaneous conditioning. L: HL
case. N: normal case. A : CS(A). X : Context.
ALPHA: associability. S: Salience. Left Panels:
NM response topography in 10 reinforced trials and
a test trial. Upper-Right Panels: Net associative
values (VT) at the end of each trial, as a function
of trials. Lower-Right Panels: Associability
(ALPHA) at 200 msec, as a function of trials.
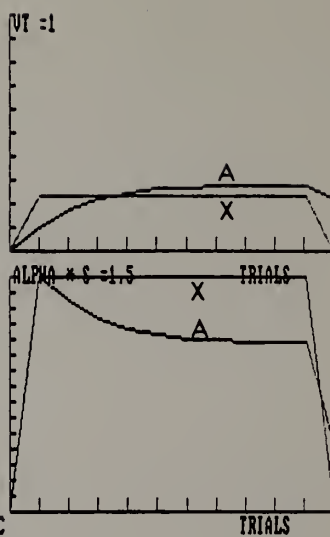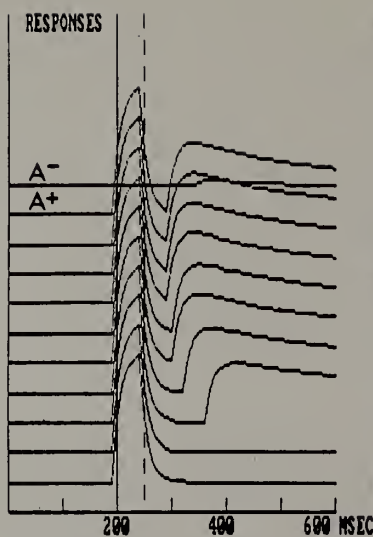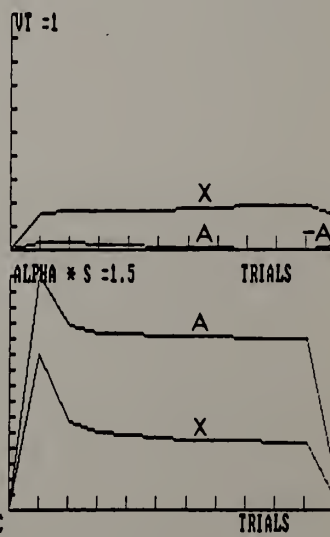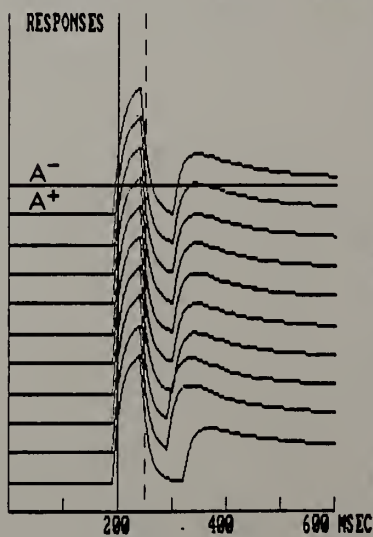
reinforced trials, but no CR occurred during the test trial. Simulations with the M-S-S model for the normal case (Fig. 3a) show that the context associability increased and CS associability decreased over trials. The small associability of the CS precluded V from increasing and therefore no CR was generated. Simulations with the S-P-H model for the normal case (Fig. 3b) show that associabilities of both the context and CS decreased over trials. For the HL case the M-S-S model showed no CR during the test trial (Fig. 3a), and the S-P-H showed only a small CR (Fig. 3b). Simulations with the M-S-S model for the HL case (Fig. 3a) show that the context associability increased and CS remained constant over trials, and CS (A) acquired inhibitory associative value. Simulations with the S-P-H model for the HL case (Fig. 3b) show that the CS associability decreased and the context associability remained constant over trials, but in both cases they were larger than the respective CS associabilities for the normal case. The CS acquired a relatively large associative value. No experimental data releveant to these simulation results are available on HL and simultaneous conditioning.

Figures 4a and 4b show simulations of a trace conditioning paradigm with a 200 msec ISI. In this paradigm, 10 simulated trials with the M-S-S model show no

Figure 4a

M-S-S model: Trace conditioning with 200 msec ISI.
L: HL case. N: normal case. A : CS(A). X :
Context. Left Panels: NM response topography in 10
reinforced trials and a test trial. Upper-Right
Panels: Net associative values (VT) at the end of
each trial, as a function of trials. Lower-Right
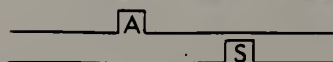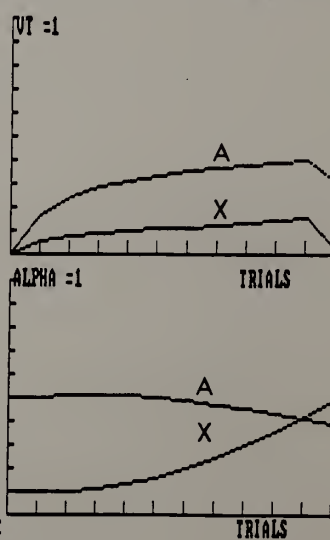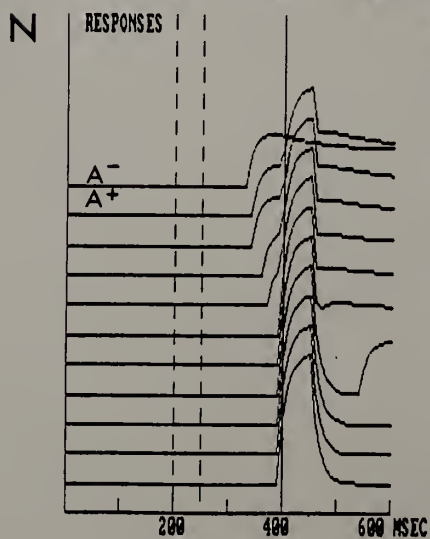Panels: Associability (ALPHA) at 400 msec, as a
function of trials.
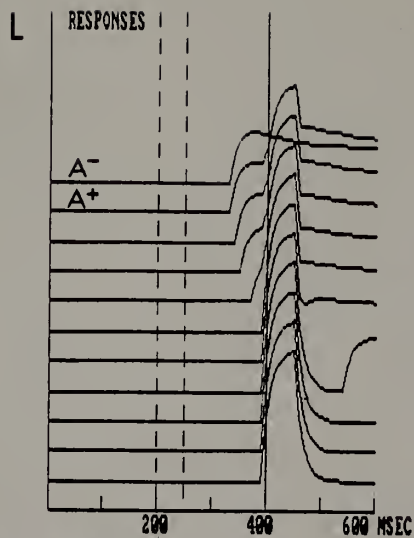
Figure 4b

S-P-H model: Trace conditioning with 200 msec ISI.
L: HL case. N: normal case. A : CS(A). X :
Context. ALPHA: associability. S: Salience. Left
Panels: NM response topography in 10 reinforced
trials and a test trial. Upper-Right Panels: Net
associative values (VT) at the end of each trial,
as a function of trials. Lower-Right Panels:
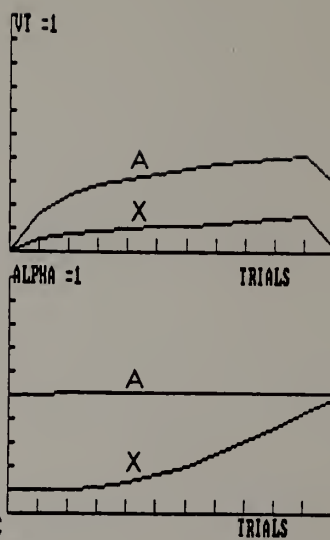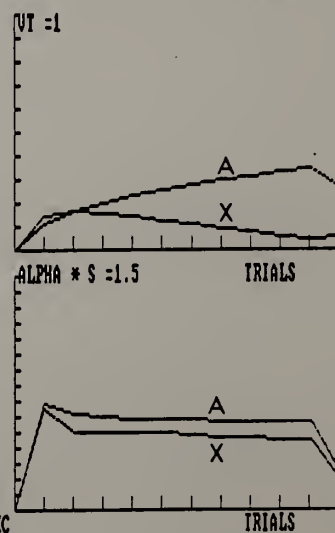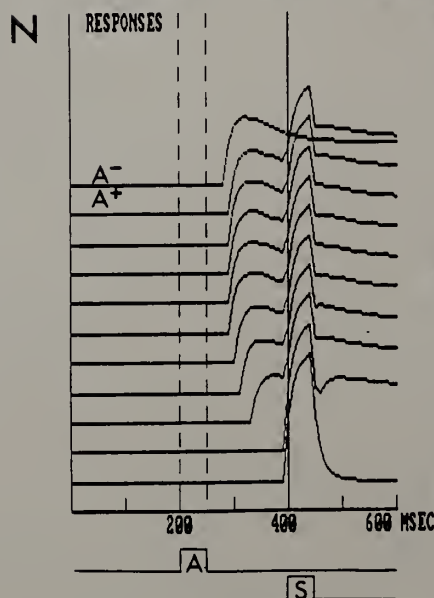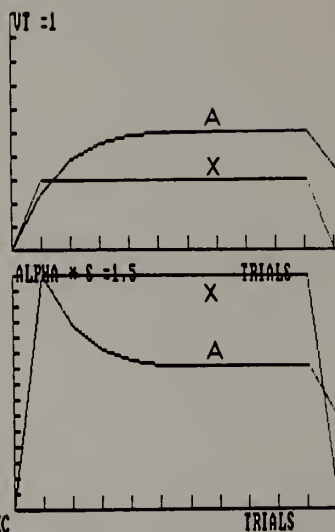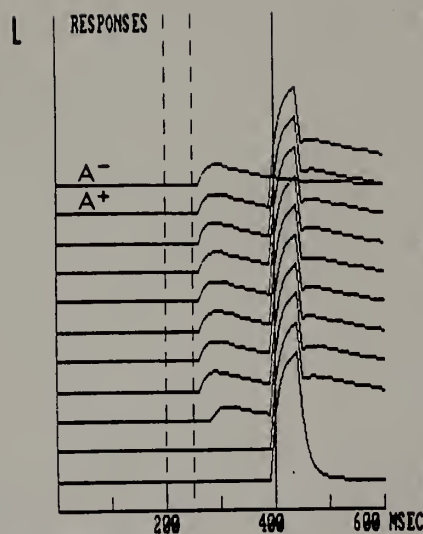Associability (ALPHA) at 400 msec, as a function of
trials.

difference for the normal and HL cases, generating CR
peaks at the point where the US occurred (Fig. 4a).
Simulations with the M-S-S model for the normal case (Fig.
4a) show that the context associability increased and CS
associability decreased over trials. In the HL case, the
CS associability remained constant over trials.
Simulations with the S-P-H model (Fig. 4b) show that in
the HL case CRs had smaller amplitude and shorter
latencies than in the normal case. Simulations with the
S-P-H model for the HL case show larger associabilities
than in the normal case.

Figures 5a and 5b show simulations of a trace
conditioning paradigm with a 300 msec ISI with the M-S-S
and S-P-H models, respectively. In this paradigm, 10
simulated trials with the M-S-S model show no conditioning
for both the normal and the HL case (Fig. 5a).
Simulations for the normal case with the S-P-H model (Fig.
5b) show interesting results. During the first trials of
training, CR onset moved towards the CS. Later on
training, as CS (A) acquired inhibitory associative value,
CR onset moved back again towards the US and finally
blended into the UR. In a sense, the context was a
predictor of the US and the CS predicted the absence of
the US during the period of the trial in which it was
presented. The combination of these predictions

Figure 5a

M-S-S model: Trace conditioning with 300 msec ISI.
L: HL case. N: normal case. A : CS(A). X :
Context. Left Panels: NM response topography in 10
reinforced trials and a test trial. Upper-Right
Panels: Net associative values (VT) at the end of
each trial, as a function of trials. Lower-Right
Panels: Associability (ALPHA) at 500 msec, as a
function of trials.

Figure 5b

S-P-H model: Trace conditioning with 300 msec ISI.
L: HL case. N: normal case. A : CS(A). X :
Context. ALPHA: associability. S: Salience. Left
Panels: NM response topography in 10 reinforced
trials and a test trial. Upper-Right Panels: Net
associative values (VT) at the end of each trial,
as a function of trials. Lower-Right Panels:
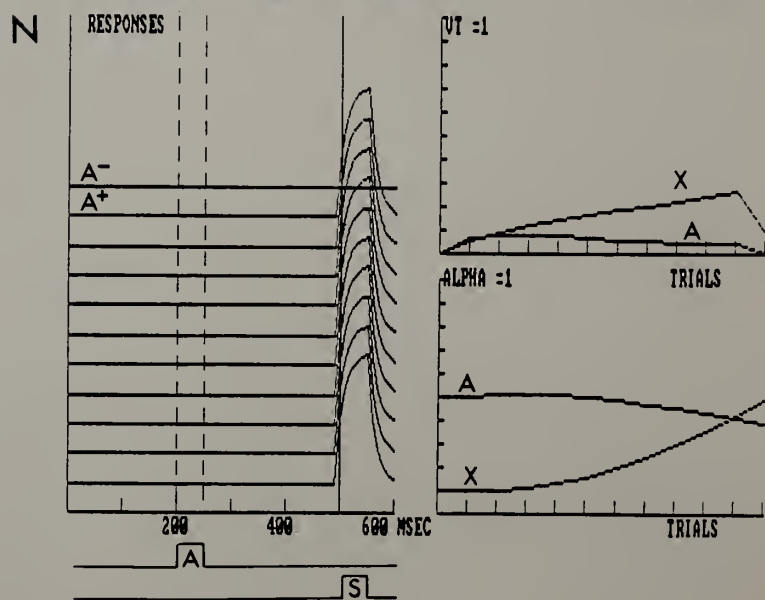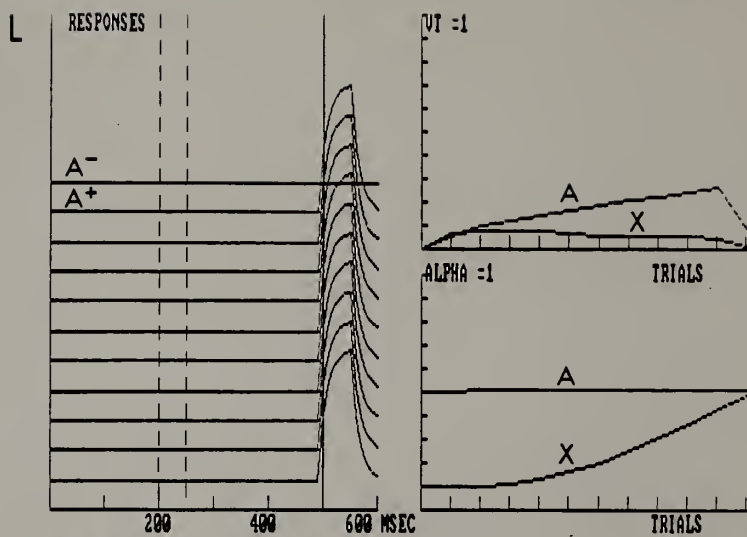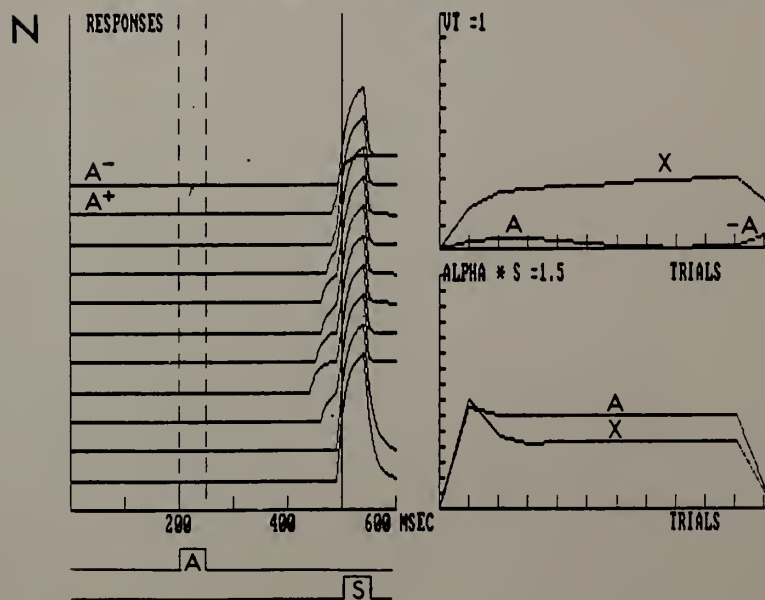Associability (ALPHA) at 500 msec, as a function of
trials.

determined that the CR blended into the UR. Simulations
for the HL case (Fig. 5b) show small CRs of short latency
that did not blend into the UR.

Taken together, the simulated data with both models
for the normal case with 0, 200 and 300 ISIs, resembled
the ISI function obtained from normal animals by Smith
(1968), Schneiderman (1966), or Schneiderman and Gormezano
(1964) in the rabbit NM preparation, with a peak at 200
msec ISI.

Figures 6a and 6b show simulations of a delay
conditioning paradigm with the M-S-S and S-P-H models,
respectively. Both models showed shorter CR latency for
the HL than for the normal case. In agreement with the
simulations, Port and Patterson (1984) report that CR
latency was shorter in animals with fimbrial lesions than
in those with cortical or sham lesions, mainly during the
first day of acquisition. Simulations with the M-S-S
model for the normal case (Fig. 6a), show that the context
associability decreased and CS associability increased
over trials. Context associability remained constant in
the HL case. Simulations with the S-P-H model for the
normal case (Fig. 6b) , show that both context and CS
associabilities decreased over trials, the CS
overshadowing the context. In the HL case both the CS's
and the contextual associabilities were larger than in the

Figure 6a

M-S-S model: Delay conditioning. L: HL case. N:
normal case. A : CS(A). X : Context. Left
Panels: NM response topography in 10 reinforced
trials. Upper-Right Panels: Net associative
values (VT) at the end of each trial, as a function
of trials. Lower-Right Panels: Associability
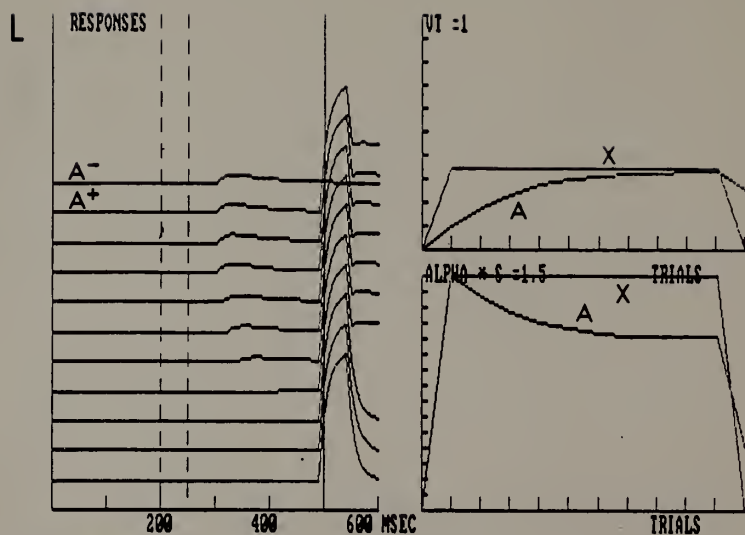(ALPHA) at 350 msec, as a function of trials.
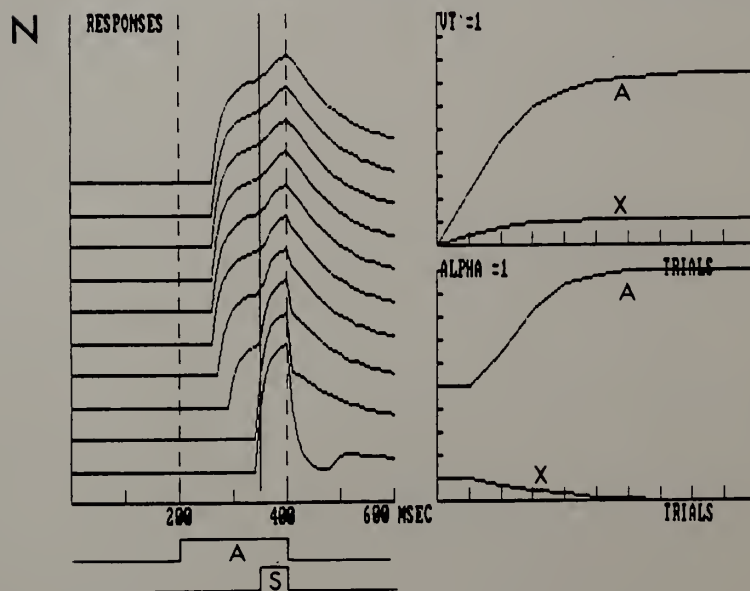
Figure 6b

S-P-H model: Delay conditioning. L: HL case. N:
normal case. A : CS(A). X : Context. ALPHA:
associability. S: Salience. Left Panels: NM
response topography in 10 reinforced trials.
Upper-Right Panels: Net associative values (VT) at
the end of each trial, as a function of trials.
Lower-Right Panels: Associability (ALPHA) at 350
msec, as a function of trials.
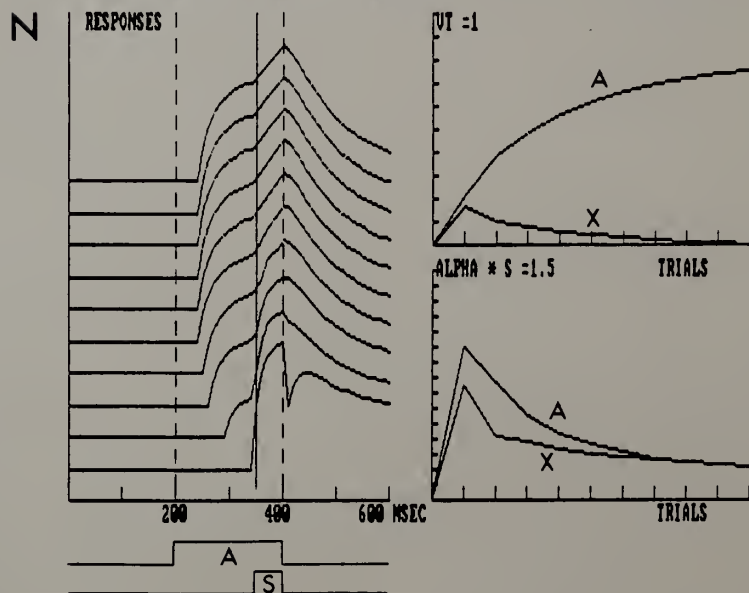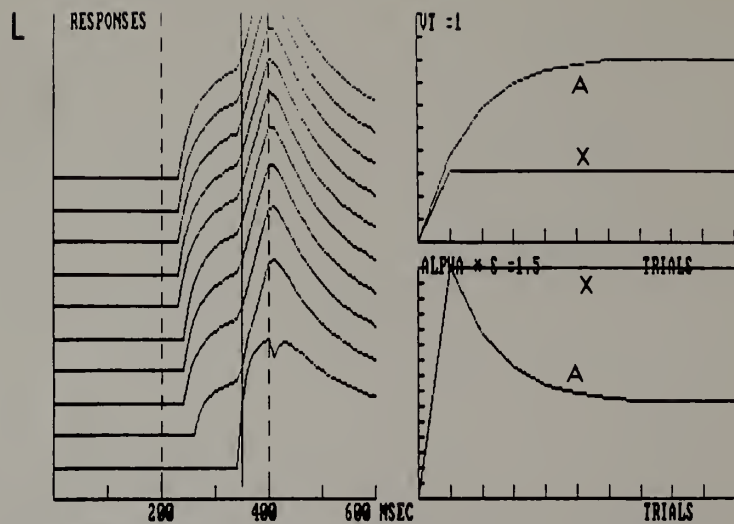
normal case and therefore both CS and context were able to acquire larger associative values than in the normal case.

Conditioned Inhibition

Experimental data.

Only one study describes the effect of HL on conditioned inhibition. Solomon (1977) presented HL and control rabbits with light CS+ trials interspersed with light-plus-tone CS- trials. He found that this procedure yields inhibitory conditioning of the tone in normal and HL animals.
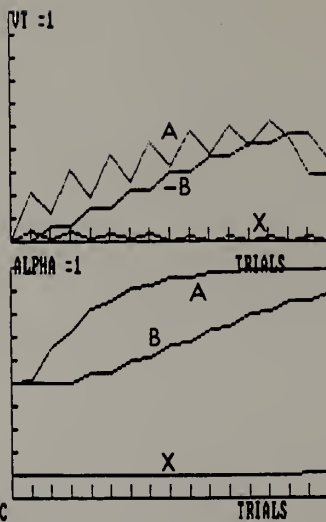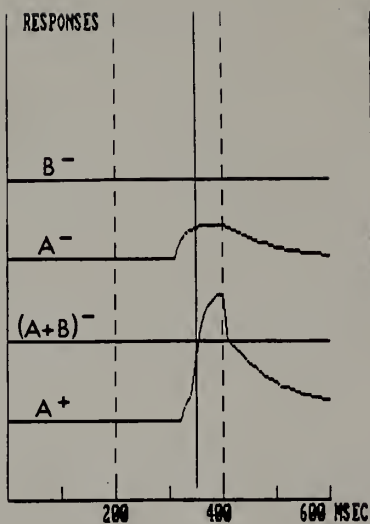
Simulation results.

Figures 7a and 7b show simulations of a conditioned inhibition paradigm with the M-S-S and S-P-H models, respectively. During conditioned inhibition two types of trials were alternated: reinforced trials consisted of a single reinforced CS (A), and nonreinforced trials consisted of a compound CS (A and B). Stimulus B was the conditioned inhibitor. After 10 simulated trials with the M-S-S model and 38 simulated trials with the S-P-H model, the CR elicited by A and B together was smaller than that elicited when A was presented alone because B has acquired inhibitory associative value. Simulations with the M-S-S

Figure 7a

M-S-S model: Conditioned Inhibition. L: HL case.
N: normal case. A : CS(A). B : CS(B). X :
Context. Left Panels: NM response topography in
A+, (A+B)-, A-, and B-trials, after 10 alternated
A+ and (A+B)- trials. Upper-Right Panels: Net
associative values (VT) at the end of each trial,
as a function of trials. Lower-Right Panels:
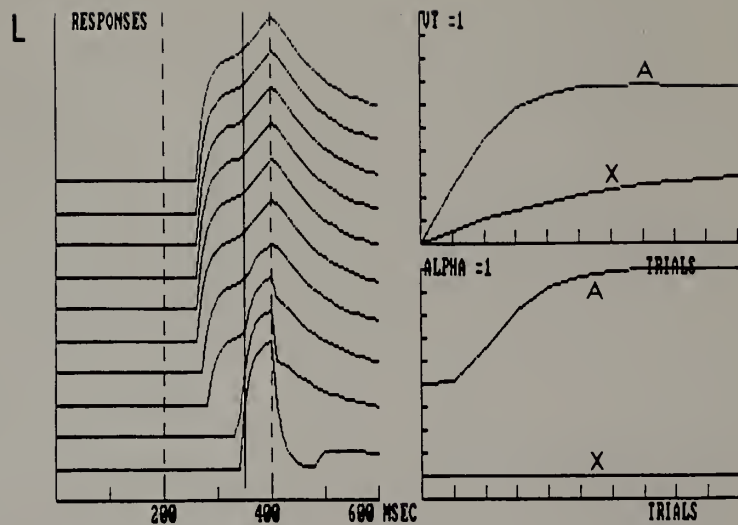Associability (ALPHA) at 350 msec, as a function of
trials.

Figure 7b

S-P-H model: Conditioned Inhibition. L: HL case.
N: normal case. A : CS(A). B : CS(B). X :
Context. ALPHA: associability. S: Salience. Left
Panels: NM response topography in A+, (A+B)-, A-,
and B-trials, after 38 alternated A+ and (A+B)-
trials. Upper-Right Panels: Net associative values
(VT) at the end of each trial, as a function of
trials. Lower-Right Panels: Associability (ALPHA)
at 350 msec, as a function of trials.
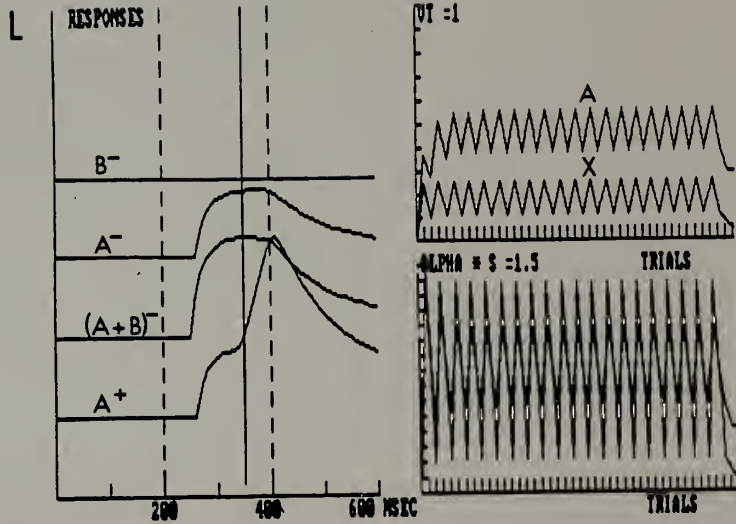
model for the normal case (Fig. 7a) show that associabilities of both CSs increased and context associability decreased over trials. Simulations for the HL case with the M-S-S model show no difference from the normal case, with the exception of a constant context associability. Simulations for the HL case with the S-P-H model (Fig. 7b) show that the CR elicited by A and B together was not smaller than that elicited when A was presented alone because B had not acquired inhibitory associative value. Simulations with the S-P-H model for the HL case show larger associabilities than the normal case. Solomon (1977) reports no impairment in conditioned inhibition for HL animals, in agreement with simulations obtained with the M-S-S model, but not with those obtained with the S-P-H model.

<u>Extinction</u>.

<u>Experimental</u> <u>data</u>.

Two studies describe the effect of HL on extinction. After initial acquisition, extinction of conditioned NM response in rabbit appeared to be unaffected by HL (Berger & Orr, 1983; Schmaltz & Theios, 1972). However, normal rabbits decreased the number of trials to reach extinction criterion whereas HL rabbits increased the number of

trials to criterion, following alternating acquisition-
reacquisition sessions (Schmaltz & Theios, 1972).

The effect of HL on NM topography has also been
studied. Orr and Berger (1985) found that HL did not
affect CR topography during extinction using a 850-msec
CS, a 100-msec air puff US, and a 750-msec ISI.

Simulation results.

Figures 8a and 8b show simulations of extinction with
the M-S-S and S-P-H models, respectively. Ten extinction
trials were simulated with initial values resulting from
simulations of 10 reinforced trials in the above-mentioned
delay conditioning paradigm. Simulations with the M-S-S
model (Fig. 8a) show that extinction proceeded faster in
the HL case than in the normal case. In the normal case
context associability was larger than zero and its
associative value decreases. In the HL case context
associability was zero and its associative value could not
decrease. Simulations with the S-P-H model (Fig. 8b)
show little difference in the rate of extinction for
normal and HL cases. Simulations with the S-P-H model for
the HL case show larger decreasing associabilities than
the normal case. Results obtained with the S-P-H, but not
with the M-S-S model, are in accordance with Berger and
Orr (1983) and with the initial extinction series of the

Figure 8a

M-S-S model: Extinction. L: HL case. N: normal
case. A : CS(A). X : Context. Left Panels: NM
response topography in 10 extinction trials.
Upper-Right Panels: Net associative values (VT) at
the end of each trial, as a function of trials.
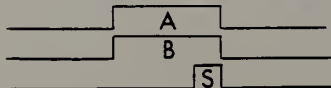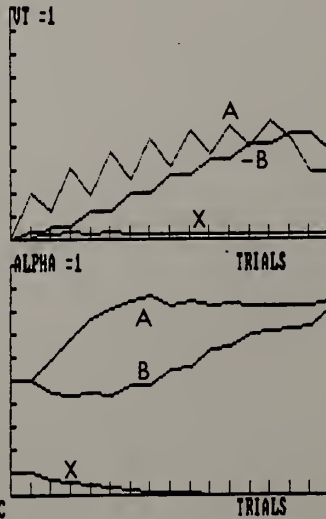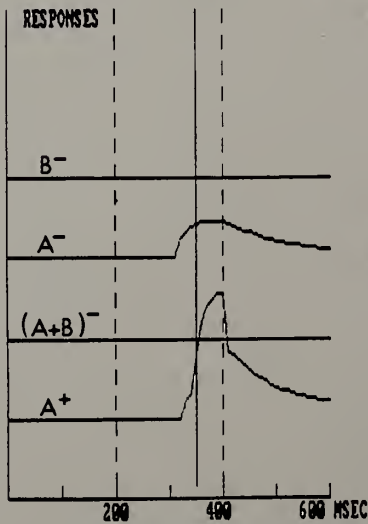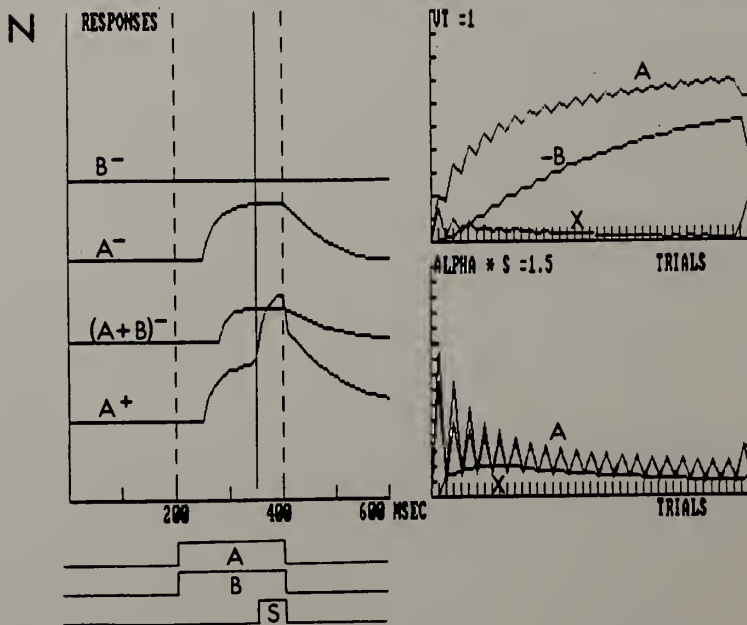Lower-Right Panels: Associability (ALPHA) at 350
msec, as a function of trials.
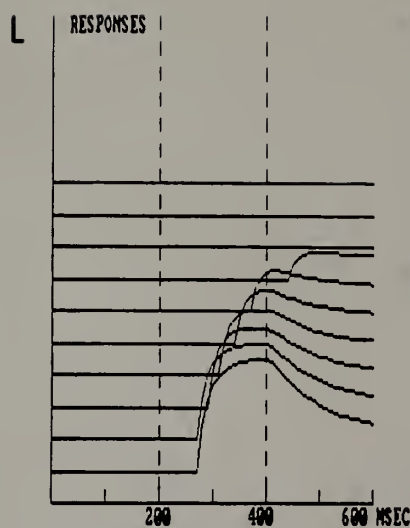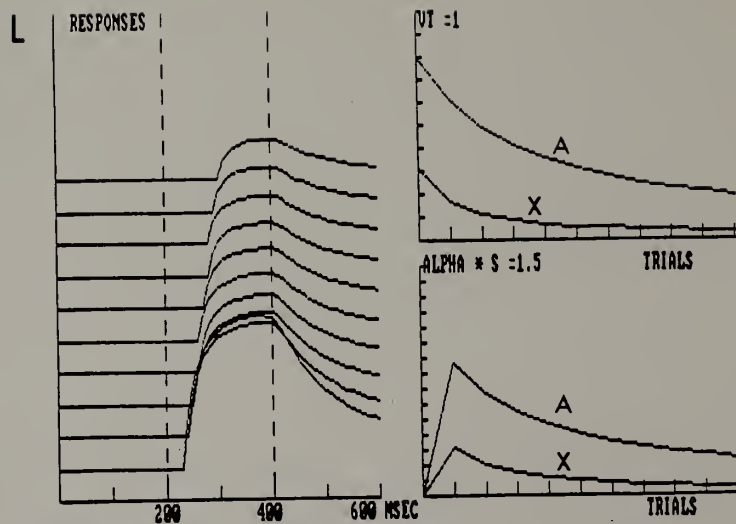
Figure 8b

S-P-H model: Extinction. L: HL case. N: normal
case. A : CS(A). X : Context. ALPHA:
associability. S: Salience. Left Panels: NM
response topography in 10 extinction trials.
Upper-Right Panels: Net associative values (VT) at
the end of each trial, as a function of trials.
Lower-Right Panels: Associability (ALPHA) at 350
msec, as a function of trials.
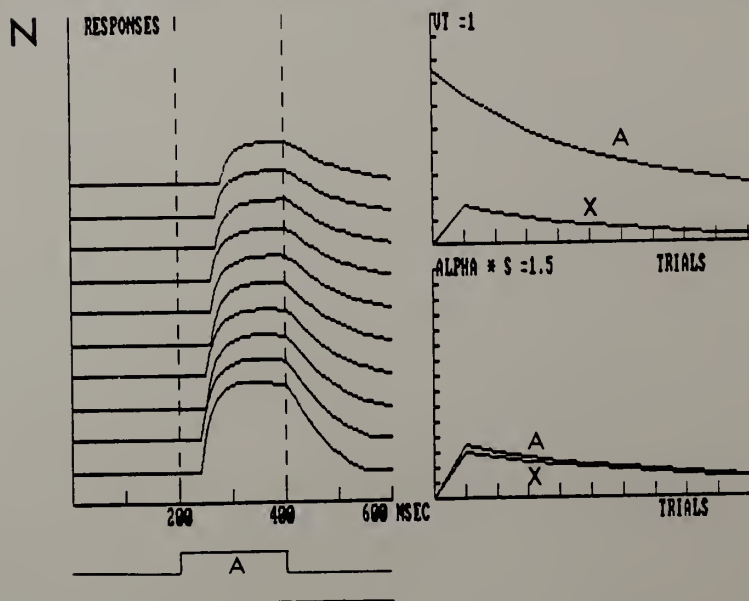
Schmaltz and Theios (1972) study.

In agreement with prediction with both the M-S-S and the S-P-H models Orr and Berger (1985) report that HL have no effect on the shape and latency of the NM responses during extinction.

Latent inhibition.

Experimental data.

The effect of HL on latent inhibition has been described in the rabbit NM preparation. Latent inhibition (LI) refers to the finding that repeatedly presenting the CS alone, before pairing it with the US, produces retardation in the acquisition of the CR. Solomon and Moore (1975) report that animals with HL showed impaired LI after preexposure to a tone CS.

Simulation results.

Figures 9a and 9c show simulations of a LI paradigm with the M-S-S and S-P-H models, respectively. Figures 9b and 9d show simulations of control groups with the M-S-S and S-P-H models, respectively. The M-S-S model makes explicit the effect of various temporal parameters on LI resulting from CS preexposure. For the normal case, the model stipulates that LI is a decreasing function of CS

duration and an increasing function of the intertrial interval (ITI) (see Moore & Stickney, 1980). With a CS of relatively brief duration, the context becomes the best predictor of the CS, and therefore the CS loses associability and LI occurs. With a CS of relatively long duration, the CS becomes a better predictor of itself than does the context, and therefore the CS gains associability and LI does not occur. In the HL case the M-S-S model does not permit LI because the associability of the preexposed CS cannot decrease.
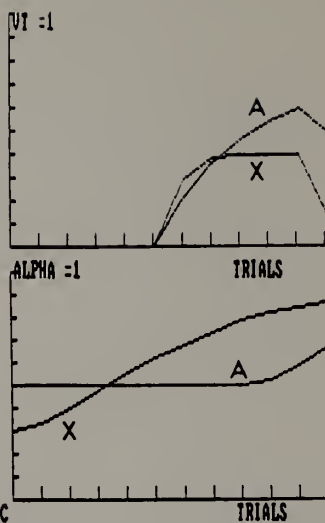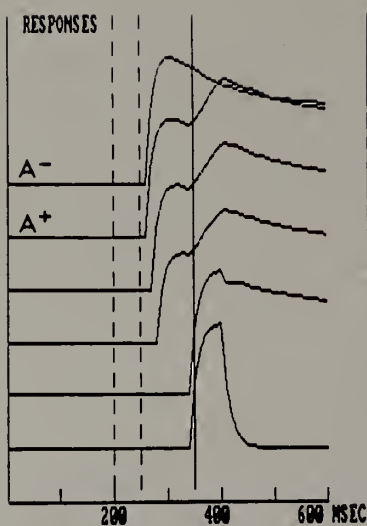
In the S-P-H model LI depends on the number of CS preexposures and its duration but neither on the CS duration nor on the ITI. This model predicts the absence of LI in the HL case because, even though the CS's salience decreases during preexposure, it decreases at a slower rate than in the normal case. Moreover, the decrease in salience is overcompensated by the increase of the CS's associability during the trials on which CS and US are paired. Therefore, simulations for HL cases under control and experimental procedures have similar CR amplitudes.

Simulations consisted of 5 trials of CS preexposure with the M-S-S model and 10 trials of CS preexposure with the S-P-H model, followed by 5 trials in which the CS is paired with the US (Figs. 9a and 9c). Control cases

Figure 9a

M-S-S model: Latent Inhibition. L: HL case. N:
normal case. A : CS(A). X : Context. Left
Panels: NM response topography in 5 CS-US trials
and a test trial after 5 CS preexposure trials.
Upper-Right Panels: Net associative values (VT) at
the end of each trial, as a function of trials.
Lower-Right Panels: Associability (ALPHA) at 350
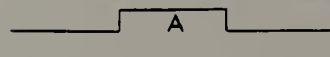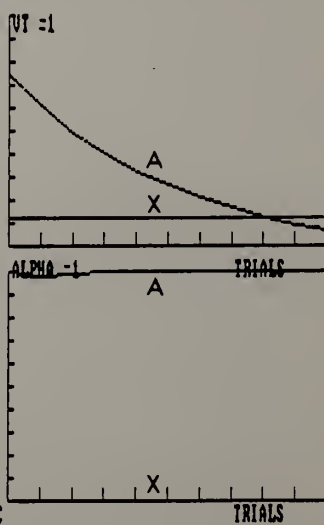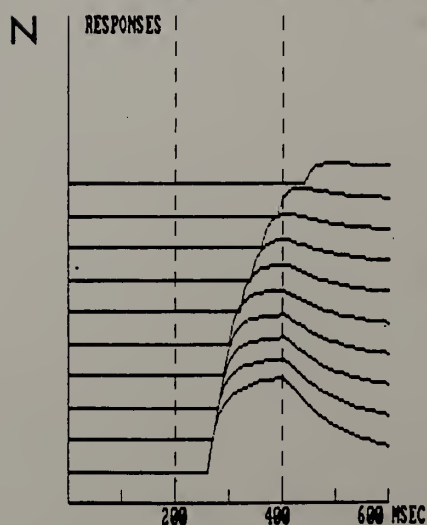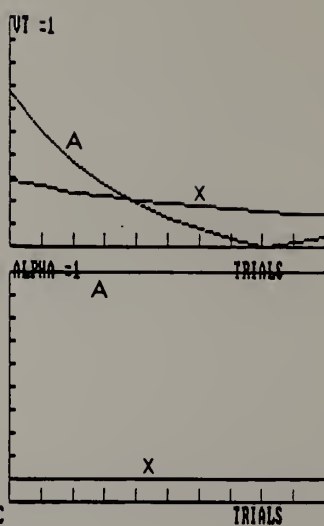msec, as a function of trials.

Figure 9b

M-S-S model: Control for Latent Inhibition. L: HL
case. N: normal case. A : CS(A). X : Context.
Left Panels: NM response topography in a CS-US
trial and a test trial after 5 context-only
preexposure trials. Upper-Right Panels: Net
associative values (VT) at the end of each trial,
as a function of trials. Lower-Right Panels:
Associability (ALPHA) at 350 msec, as a function of
trials.
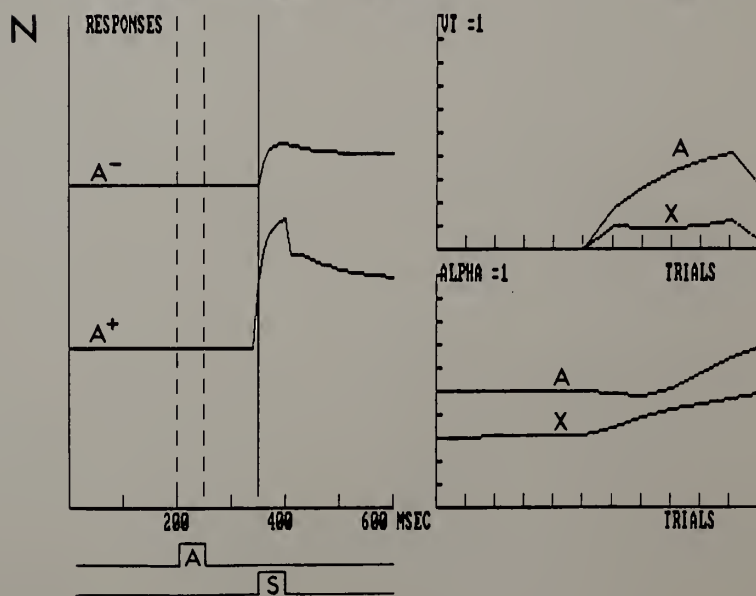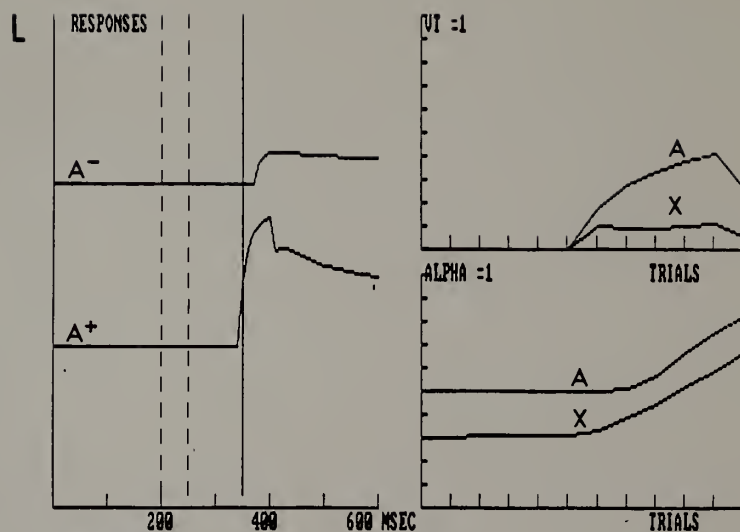
received 5 or 10 context-only trials followed by the 5 CS-US trials (Figs. 9b and 9d). The CS was 50 msec with the M-S-S model and 200 msec with the S-P-H model. CSs longer than 100 msec did not yield LI with the M-S-S model. US duration was 50 msec and the ISI 200 msec with both models.

Simulations with the M-S-S model for the normal case show that the context associability increased and CS associability decreased over CS preexposure trials, and this process was reversed during reinforced trials. The decreased associability caused the CS to acquire associative value slower than in the control case (see Fig. 9b) and to generate a smaller CR on the sixth trial.

In the HL case simulations with the M-S-S model show that the context associability increased but CS associability remained constant over CS preexposure trials, and both associabilities increased during reinforced trials. Because of its increased associability the context acquired higher associative value than in the control case, and CRs were generated earlier in the HL than in the normal case. In the HL case the M-S-S model generated a larger CR in the sixth trial after CS-preexposure, than after context-only preexposure (Fig. 9b).

Simulations with the S-P-H model for the normal case

Figure 9c

S-P-H model: Latent Inhibition. L: HL case. N:
normal case. A : CS(A). X : Context. ALPHA:
associability. S: Salience. Left Panels: NM
response topography in 5 CS-US trials after 10 CS
preexposure trials. Upper-Right Panels: Net
associative values (VT) at the end of each trial,
as a function of trials. Lower-Right Panels:
Associability (ALPHA) at 350 msec, as a function of
trials.
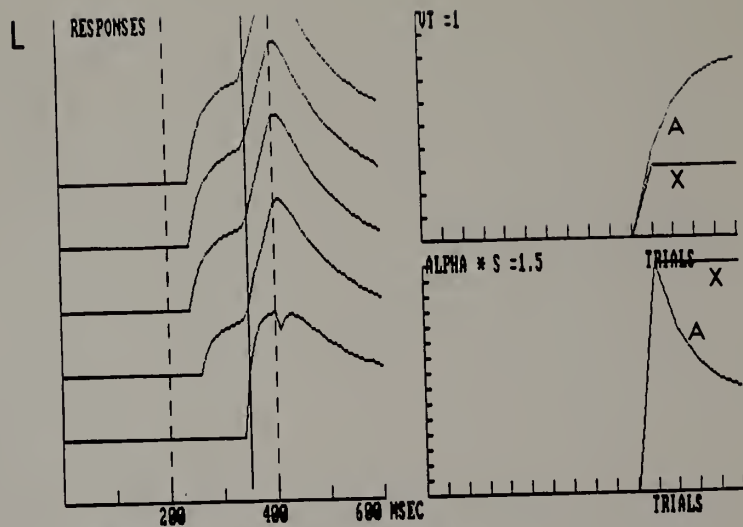
Figure 9d

S-P-H model: Control for Latent Inhibition. L: HL
case. N: normal case. A : CS(A). X : Context.
ALPHA: associability. S: Salience. Left Panels:
NM response topography in 5 CS-US trials after 10
context-only preexposure trials. Upper-Right
Panels: Net associative values (VT) at the end of
each trial, as a function of trials. Lower-Right
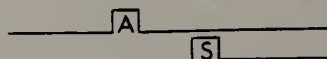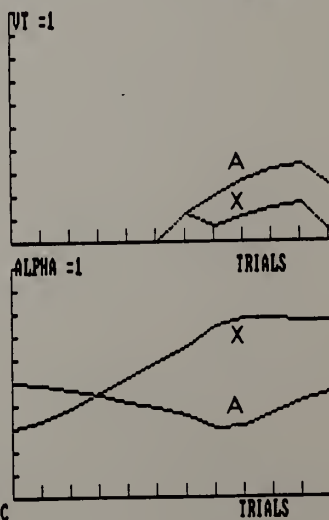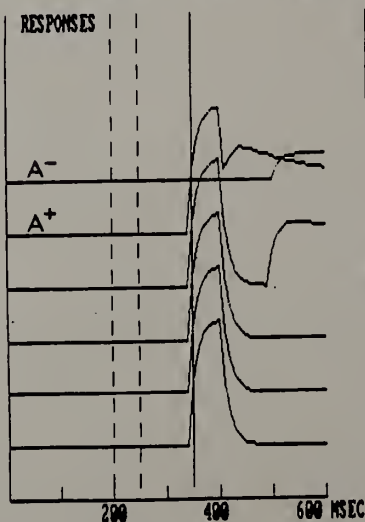Panels: Associability (ALPHA) at 350 msec, as a
function of trials.

show that the context and CS saliences decreased over CS preexposure trials. The decreased salience caused the CS to acquire associative value slower than in the control case (see Figs. 9c and 9d) and to generate CRs in later trials. In the HL case simulations with the S-P-H model show that the context and CS associabilities were larger than in the normal case. Because of its increased associability the context acquired higher associative value than in the control case, and CRs were generated earlier in the HL than in the normal case. Both models are consistent with Solomon and Moore (1975), showing not only absence of LI, but also that CS preexposure facilitates acquisition during reinforced trials in the HL case.

Blocking and mutual overshadowing.

Experimental data.

In blocking, an animal is first conditioned to a CS(A), and this training is followed by conditioning to a compound consisting of A and a second stimulus B. This procedure results in a weaker conditioning to B. Solomon (1977) found that HL disrupted blocking of the rabbit NM response. Control groups in Solomon's (1977) investigation provide evidence regarding the effect of HL

on mutual overshadowing between two compounded CSs of differential salience. Unlike in the case of blocking, HL rabbits showed no deficit in mutual overshadowing.

Simulation results.

Figures 10a and 10b show simulations of a blocking paradigm with the M-S-S and S-P-H models, respectively. Experimentals received 5 trials with one CS (blocker) paired with the US followed by 5 trials with the same CS and a second (blocked CS) paired with the US. Controls received 5 two-CS trials in which both CSs were presented together and paired with the US (A in Fig. 11a and 11b). Controls were subject to mutual overshadowing between the two component CSs. Figure 10a and 10b show that both models simulated blocking in the normal case because the CR for the blocked CS was smaller in the experimental condition than in the control conditions shown in Figs. 11a and 11b, respectively. The blocking effect was more clear for the M-S-S model. Consistent with Solomon (1977), simulations with both models show that HL virtually eliminated blocking. In the M-S-S model the blocked CS did not lose associability in the HL case and therefore was able to achieve a high V. In the S-P-H model the blocked CS's associability ($\alpha = |\lambda^{US} - V_i^{\cdot US}|$) was larger in the HL case than in the normal case ($\alpha = |\lambda^{US} - $

Figure 10a

M-S-S model: Blocking. L: HL case. N: normal
case. A : CS(A). B : CS(B). X : Context. Left
Panels: NM response topography in A-and B-test
trials, after 5 CS(A) reinforced trials and 5 CS(A)
and CS(B) reinforced trials. Upper-Right Panels:
Net associative values (VT) at the end of each
trial, as a function of trials. Lower-Right
Panels: Associability (ALPHA) at 350 msec, as a
function of trials.

Figure 10b

S-P-H model: Blocking. L: HL case. N: normal case.
A : CS(A). B : CS(B). X : Context. ALPHA:
associability. S: Salience. Left Panels: NM
response topography in A-and B- test trials, after
5 CS(A) reinforced trials and 5 CS(A) and CS(B)
reinforced trials. Upper-Right Panels: Net
associative values (VT) at the end of each trial,
as a function of trials. Lower-Right Panels:
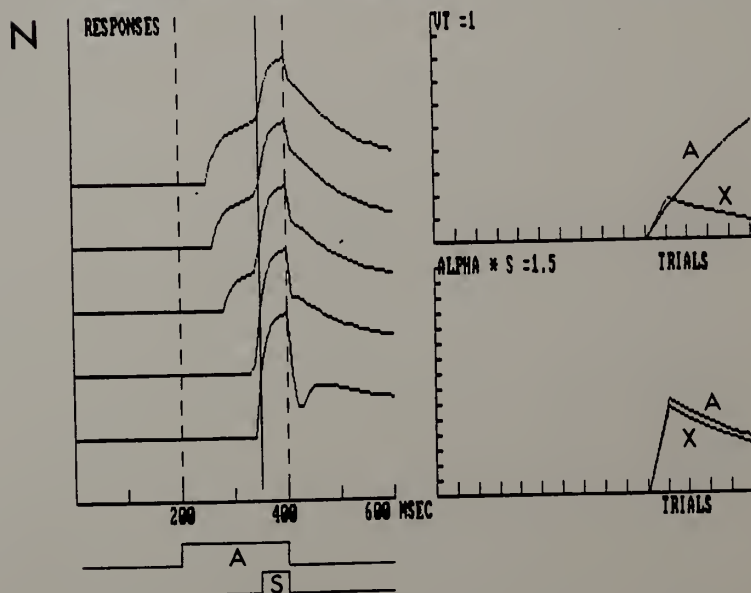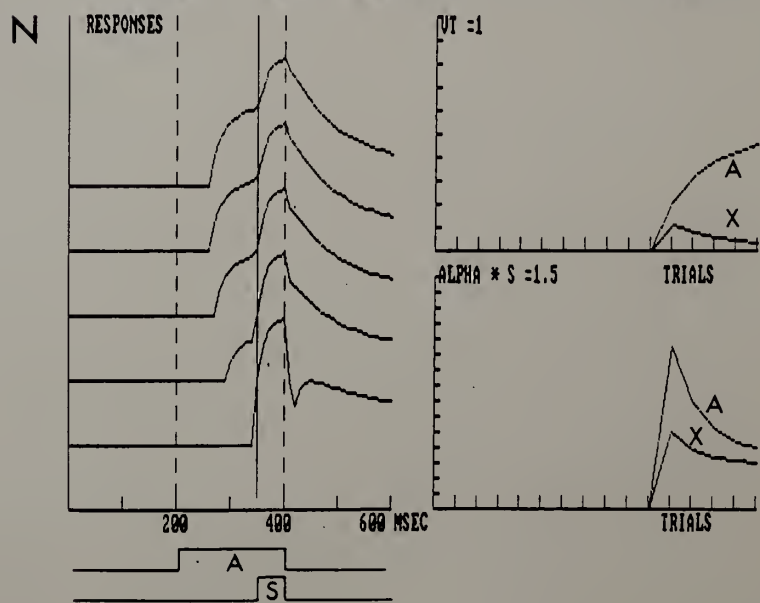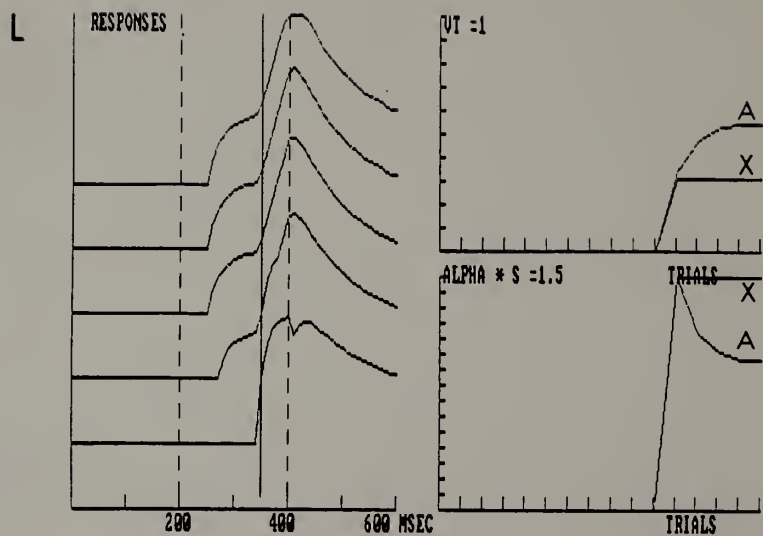Associability (ALPHA) at 350 msec, as a function of
trials.
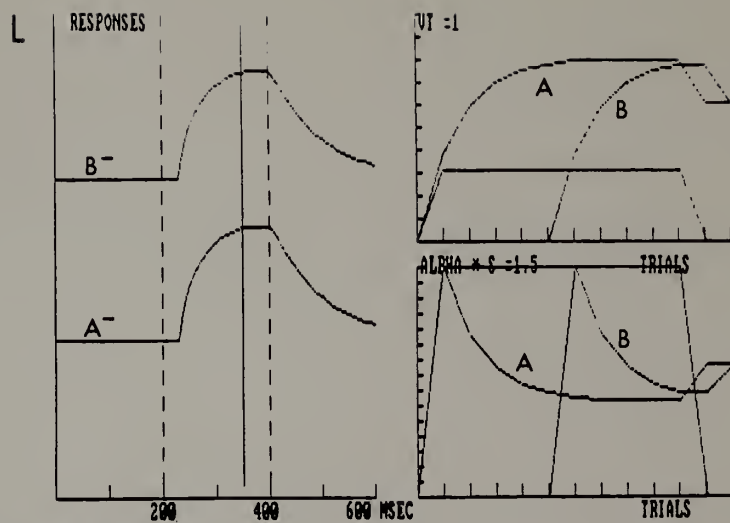
B^{US}).

Figures 11a and 11b show simulations of a mutual overshadowing paradigm with the M-S-S and S-P-H models, respectively. The paradigm consisted of reinforced presentations of CS(A) and CS(B) together. In both the normal and HL cases, CRs elicited by A in Fig. 11a were smaller than CRs in Fig. 6a where CS(A) has been reinforced alone, i.e., the M-S-S model yielded mutual overshadowing of CS(A) in both the normal and HL cases. HL did not affect mutual overshadowing because both CSs had the same initial value of associability. They therefore accumulated V at the same rate, but without the increase in associability that occurred when a single CS was paired with the US. Had the blocked CS a lower initial associability than the blocker, HL would have prevented mutual overshadowing. Comparing CRs elicited by A in Fig. 11b with CRs in Fig. 6b where CS(A) has been reinforced alone, shows that the S-P-H model yielded mutual overshadowing of CS(A) in the normal case. HL did affect mutual overshadowing because CS(A) associability was not influenced by either the context or the blocker. Solomon (1977) found that mutual overshadowing was not affected in HL rabbits, supporting the M-S-S but not the S-P-H results.

Figure 11a

M-S-S model: Mutual overshadowing. L: HL case. N:
normal case. A : CS(A). B : CS(B). X : Context.
Left Panels: NM response topography in A- and B-
test trials, after 5 CS(A) and CS(B) reinforced
trials. Upper-Right Panels: Net associative values
(VT) at the end of each trial, as a function of
trials. Lower-Right Panels: Associability (ALPHA)
at 350 msec, as a function of trials.
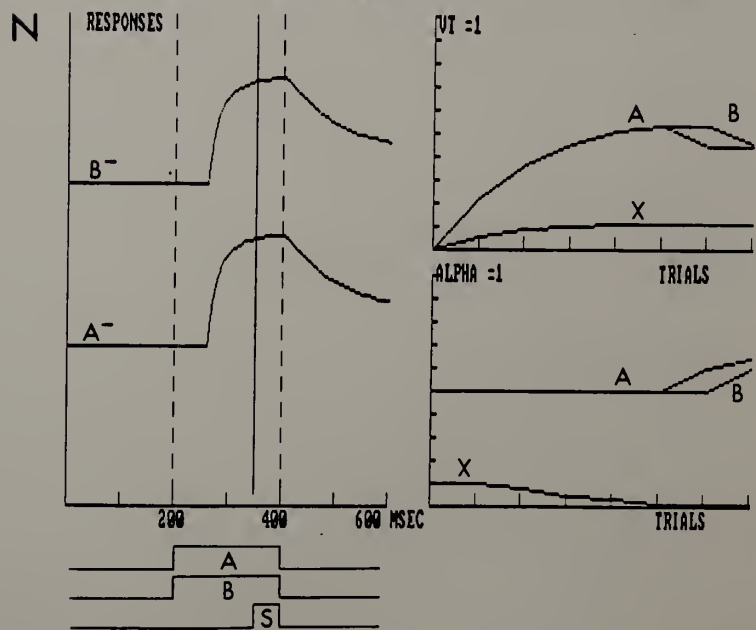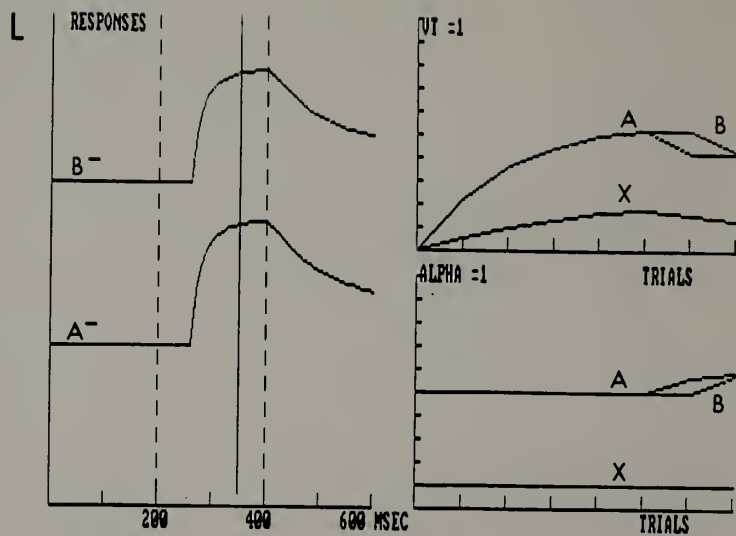
Figure 11b

S-P-H model: Mutual overshadowing. L: HL case. N:
normal case. A : CS(A). B : CS(B). X : Context.
ALPHA: associability. S: Salience. Left Panels:
NM response topography in A- and B-test trials,
after 5 CS(A) and CS(B) reinforced trials. Upper-
Right Panels: Net associative values (VT) at the
end of each trial, as a function of trials. Lower-
Right Panels: Associability (ALPHA) at 350 msec, as
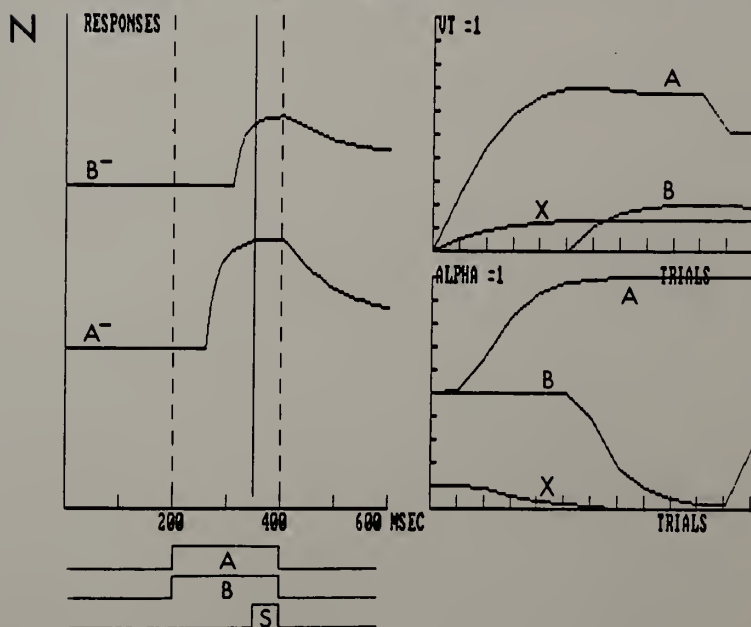a function of trials.

Discrimination reversal

Experimental data.

The effect of HL on discrimination reversal has been studied in the NM and eyelid preparations in the rabbit. Buchanan and Powell (1980) examined the effect of HL on acquisition and reversal of eyeblink discrimination in rabbits. HL slightly impaired acquisition of discrimination and severely disrupted its reversal by increasing responding to CS-. Berger and Orr (1983) contrasted HL and control rabbits in two-tone differential conditioning and reversal of the rabbit NM response. Although HL did not affect initial differential conditioning, these animals were incapable of suppressing CRs to the original CS+ after it assumed the role of CS-. This was true even following extended training.

The effect of HL on NM topography in a discirmination reveral paradigm has been studied. Orr and Berger (1985) report that HL affects CR topography in a discrimination reversal task but not during the discrimination acquisition using an 850-msec CS, a 100-msec air puff US, and a 750-msec ISI. On the last trials of reversal, HL animals showed greater peak NM amplitude and greater area under the NM response curve during the CS period, with both the CS+ and the CS-. Control and HL animals differed

in latency to NM onset, latency to peak NM, and UCS area only on the first reversal trials.

Simulation results.

Figures 12a and 12b show simulations of a discrimination reversal paradigm with the M-S-S and S-P-H models, respectively. In the differential conditioning phase, 9 reinforced trials with one CS(A) alternated with 9 nonreinforced trials with a second CS(B). During reversal, the original nonreinforced CS(B) was reinforced for 9 trials; these trials alternated with 9 trials in which CS(A), the reinforced CS in the first phase, was presented without the US.

Simulations with the M-S-S model (Fig. 12a) show that after differential conditioning, Vs for each CS were virtually the same for normal and HL cases. Context associability was zero in the normal case and larger than zero in the HL case. After differential conditioning V for A was higher than V for B, which had become inhibitory. After reversal, V for B increased to approximately the same level achieved by A during differential conditioning. At the same time, V for A became inhibitory as a consequence of the nonreinforced trials. After reversal, CRs for each CS were virtually the same for normal and HL cases. CS(A) attained larger

Figure 12a

M-S-S model: Discrimination reversal. L: HL case.
N: normal case. A : CS(A). B : CS(B). X :
Context. Left Panels: NM response topography in A-
, B+, B-, and (A+B)-trials, after 9 CS(B)
reinforced trials and 9 CS(A) nonreinforced trials.
Upper-Right Panels: Net associative values (VT) at
the end of each trial, as a function of trials.
Lower-Right Panels: Associability (ALPHA) at 350
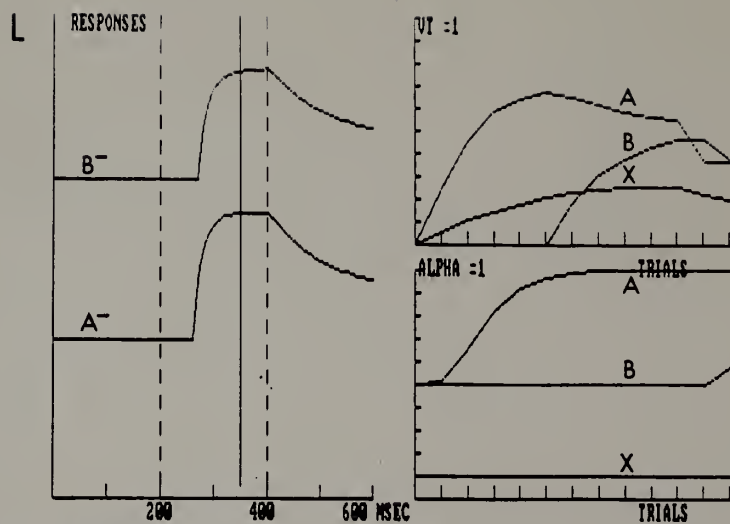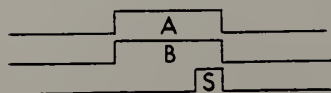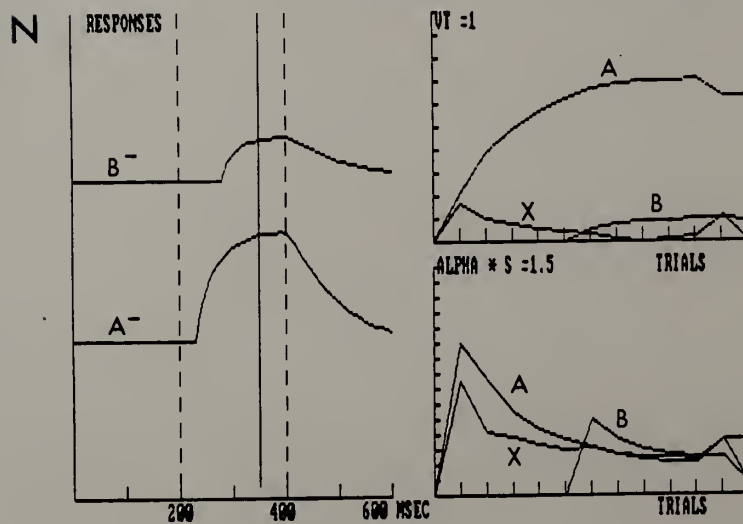msec, as a function of trials.
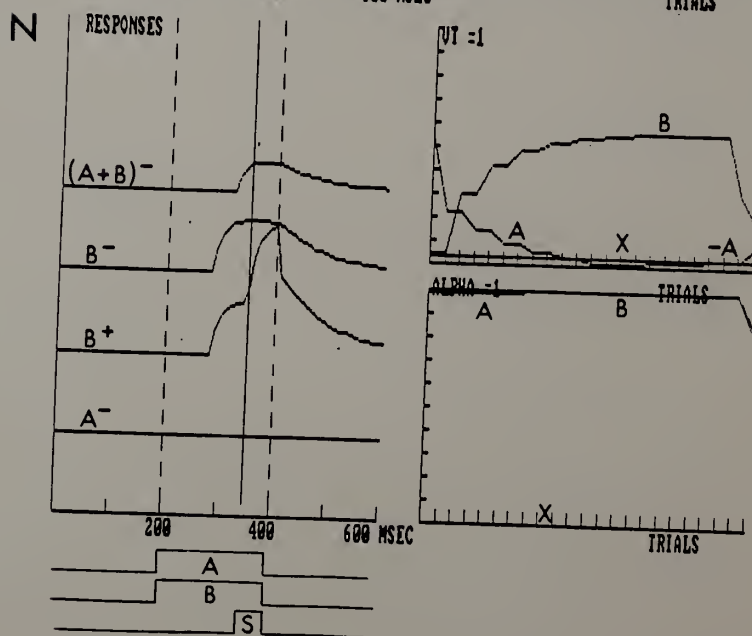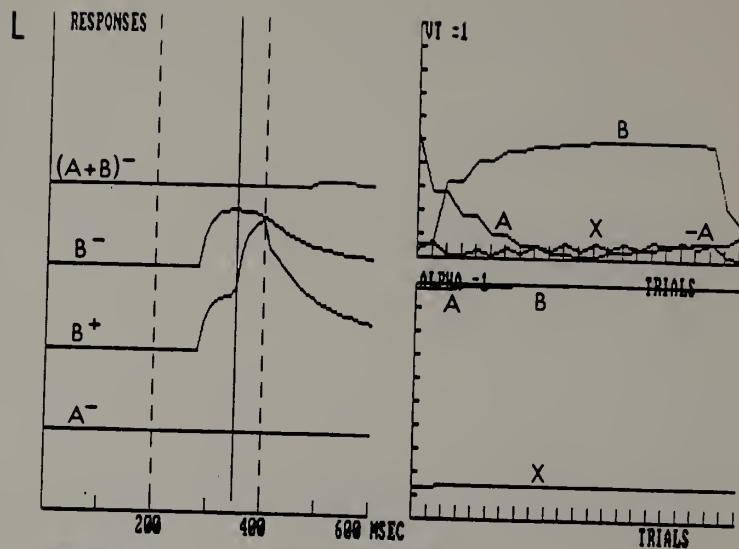
Figure 12b

S-P-H model: Discrimination reversal. L: HL case.
N: normal case. A : CS(A). B : CS(B). X :
Context. ALPHA: associability. S: Salience. Left
Panels: NM response topography in A-, B+, B-, and
(A+B)-trials, after 9 CS(B) reinforced trials and 9
CS(A) nonreinforced trials. Upper-Right Panels:
Net associative values (VT) at the end of each
trial, as a function of trials. Lower-Right
Panels: Associability (ALPHA) at 350 msec, as a
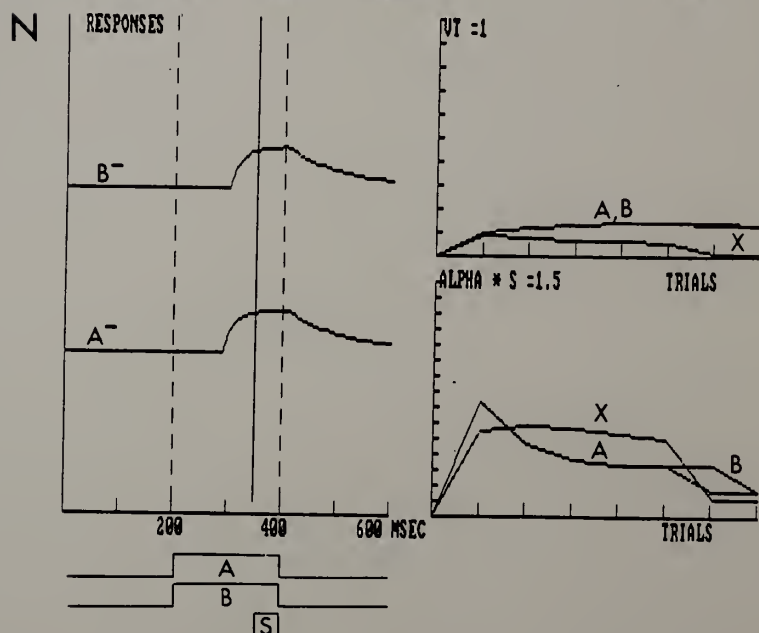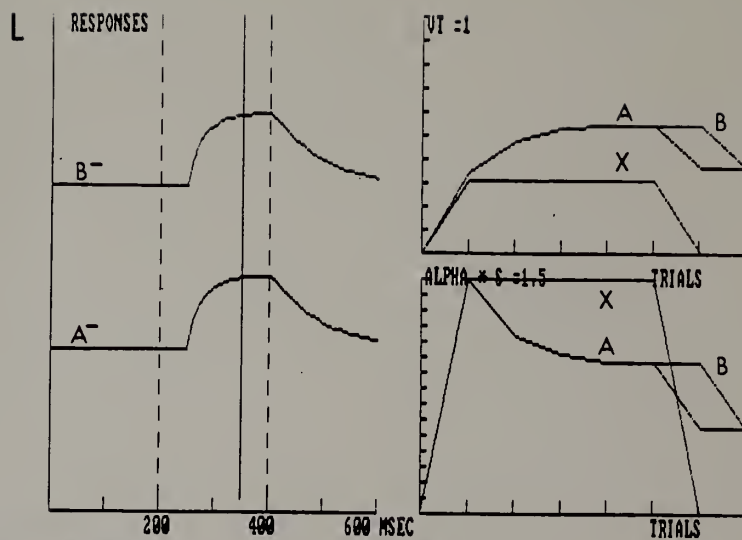function of trials.
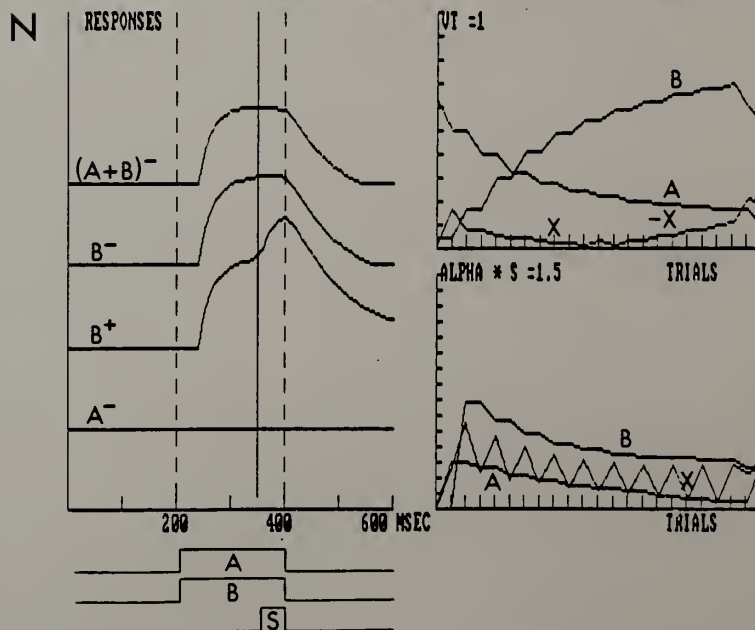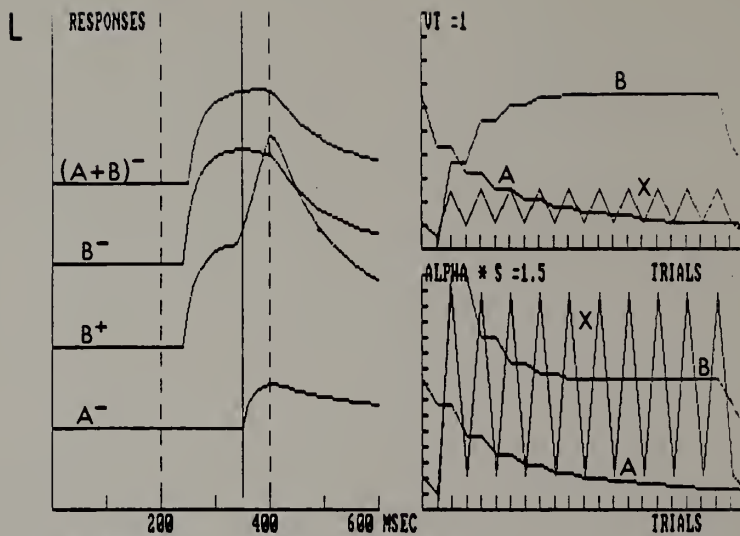
inhibitory associative value in the HL case than in the
normal case, and this was manifested by the small CR
produced by CS(A) and CS(B) when presented together.

Simulations with the S-P-H model (Fig. 12b) show that
after differential conditioning, A attained a higher V in
the HL case than in the normal case. The V for B became
inhibitory in the normal case and zero in the HL case.
After reversal in the normal case, V for the previously
nonreinforced CS(B) increased, and this increase was
accompanied by a corresponding decrease of V for the
previously reinforced CS(A). After reversal in the HL
case, V for the context was higher than in the normal case
because it is not overshadowed by either CS(A) or (B).
This excitatory associative value of the context allowed
CS(A) to elicit a CR even after the reversal of the
discrimination. Given that Berger and Orr (1983) and
Buchanan and Powell (1980) report high levels of
conditioned responding to both reinforced and
nonreinforced CSs after extended reversal training in HL
animals, it would appear that the S-P-H model renders the
more realistic portrayal of these data.

Simulations with the M-S-S model (Fig. 12a) show no
differences in NM amplitude and area under the NM response
curve during the CS period on the last trials of reversal,
with both the CS+ and CS-. Simulations with the S-P-H

model (Fig. 12b) show greater NM amplitude and area under the NM response curve during the CS period on the last trials of reversal, with both the CS+ and CS-. Orr and Berger (1985) report that on the last trials of a discrimination reversal task, HL animals showed greater peak NM amplitude and greater area under the NM response curve during the CS period with both the CS+ and the CS-. Simulations with the S-P-H model, but not with the M-S-S model, are in agreement with Orr and Berger's (1985) results.

Sensory preconditioning.

Experimental data.

Port and Paterson (1984) presented control rabbits and rabbits with fimbrial lesions, with tone and light CS- trials followed by light CS+ trials. This procedure yielded excitatory conditioning of the tone in normal animals but not in rabbits with fimbrial lesions.

Simulation results.

Figures 13a and 13b show simulations of a sensory preconditioning paradigm with the M-S-S and S-P-H models, respectively. In the first phase, 5 nonreinforced trials with a compound CS(A and B). During the second phase, one

Figure 13a

M-S-S model: Sensory preconditioning. L: HL case.
N: normal case. A : CS(A). B : CS(B). X :
Context. Left Panels: NM response topography in A+
and B-trials, after 5 CS(A) and CS(B) nonreinforced
trials and 5 CS(A) reinforced trials. Upper-Right
Panels: Net associative values (VT) at the end of
each trial, as a function of trials. Lower-Right
Panels: Associability (ALPHA) at 350 msec, as a
function of trials.
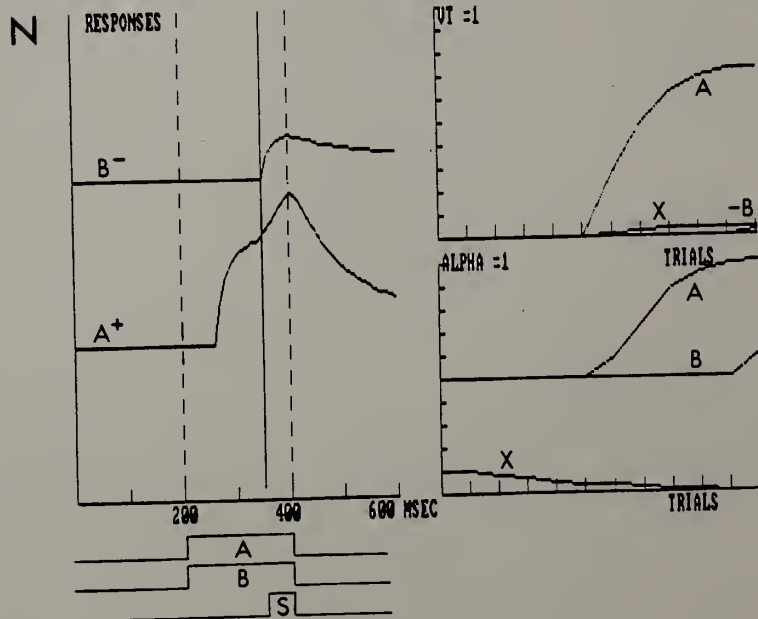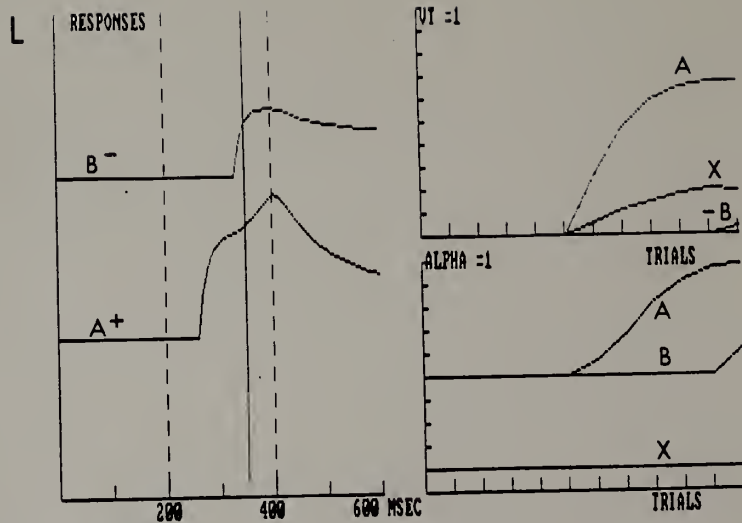
Figure 13b

S-P-H model: Sensory preconditioning. L: HL case.
N: normal case. A : CS(A). B : CS(B). X :
Context. ALPHA: associability. S: Salience. Left
Panels: NM response topography in A+ and B-trials,
after 5 CS(A) and CS(B) nonreinforced trials and 5
CS(A) reinforced trials. Upper-Right Panels: Net
associative values (VT) at the end of each trial,
as a function of trials. Lower-Right Panels:
Associability (ALPHA) at 350 msec, as a function of
trials.
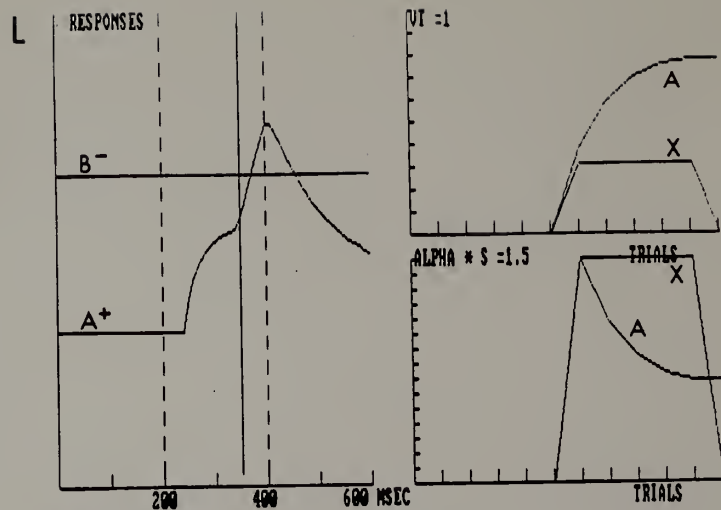
of the nonreinforced CSs (A) was reinforced for 5 trials.
A test trial assessed the CR to CS(B), which was never
paired with the US. Simulations with the M-S-S model
(Fig. 13a) show that context associability decreases
during preconditioning in the normal case but not in the
HL case. In the nonreinforced test trial, CS(B) acquired
inhibitory associative value because it was presented in a
context with excitatory associative value. CS(B)
generated a CR in both normal and HL cases. Simulations
with the S-P-H model (Fig. 13b) show that CS(B) generated
a CR in the normal but not in the HL case. Port and
Patterson (1984) found that fimbrial lesions eliminate the
responses to CS(B), a result in agreement with the
simulations with the S-P-H but not the M-S-S model.

Hippocampal neuronal activity
during classical conditioning.

Experimental data.

Hippocampal activity during classical conditioning of
the NM response is positively correlated with the
topography of the NM response. During acquisition,
increments in hippocampal unit activity precedes the
acquisition of NM CR by over 100 trials (Berger, Alger,
and Thompson, 1976). More specifically, Berger, Rinaldi,
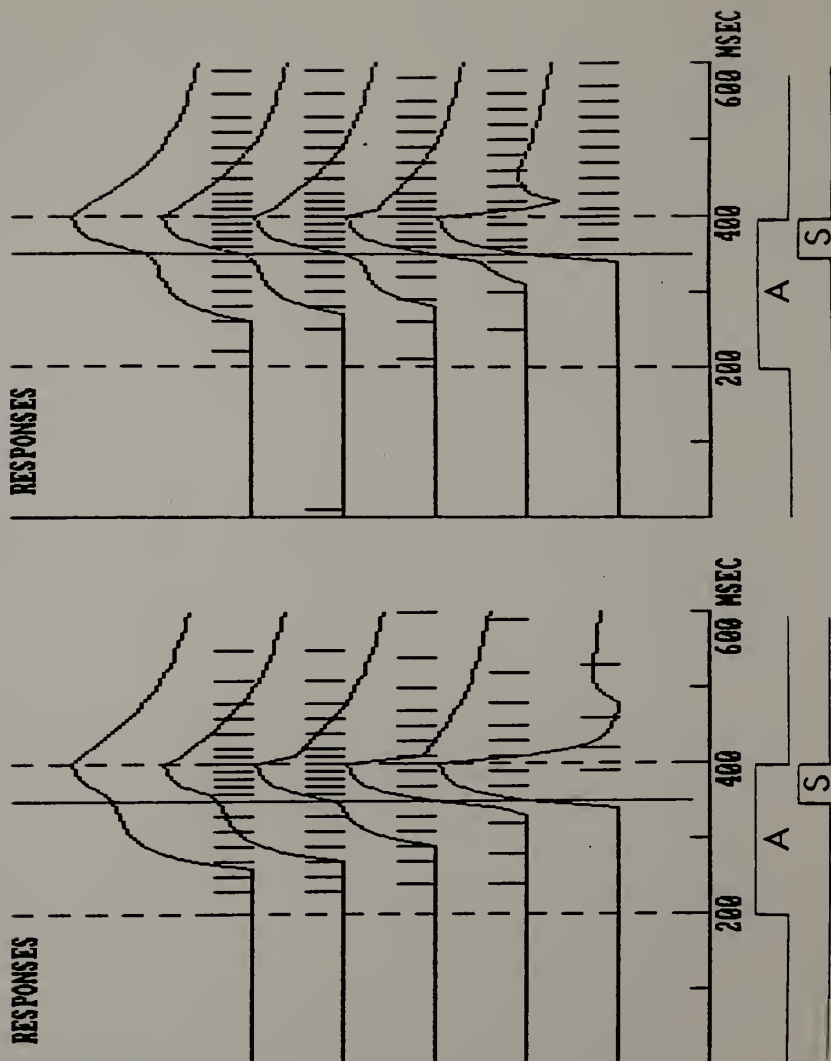
Weisz, and Thompson (1983) found that pyramidal cells were characterize by an increase in frequency of firing over conditioning trials, and by a within-trial pattern of discharge that models the NM response. Lesions of the dentate and interpositus cerebellar nuclei ipsilateral to the trained eye caused abolition of both the NM CR and the conditioned increases in hippocampal CA1 neural activity evoked by the CS (Clark, McCormick, Lavond, and Thompson, 1984).

Simulation results.

    Figure 14 shows simulations of single unit recordings obtained from the hippocampus during classical conditioning with the M-S-S and S-P-H models. It was assumed that the frequency of pyramidal firing was proportional to $\overset{.}{V}_L^{US}$ or B^{US}, in the M-S-S and S-P-H models, respectively. According to both models unit activity in the hippocampus increases during the US period within every trial, and across trials during acquisition. With both models hippocampal activity during the CS period preceded behavioral expression of the learned association. This result is explained because the behavioral response occurred only after the threshold L1 was exceeded according to Equation 20. Both models rendered realistic simulations of single unit recordings obtained from

Figure 14

Hippocampal activity during delay conditioning. NM
response topography and hippocampal single unit
activity during 5 reinforced trials. Left Panel:
M-S-S model. Right Panel: S-P-H model.

pyramidal cells during acquisition of classical
conditioning (Berger, et al., 1983).

Acquisition after hippocampal stimulation.

Experimental data.

    Berger (1984) found that entorhinal cortex
stimulation that produced long-term potentiation (LTP)
increased the rate of acquisition of classical
conditioning of the rabbit NM response. Berger (1984)
suggested that LTP might enhance the rate of conditioning
by enhancing the rate at which hippocampal unit activity
increases during acquisition. Post-trial subseizure-level
electrical stimulation of the dorsal hippocampus resulted
in a facilitation of NM response conditioning (Prokasy,
Kesner, and Calder, 1983). Prokasy et al. (1983)
suggested that the effect would be mediated by the
activation of midbrain and cerebellar circuits.

Simulation results.

    Figures 15a and 15b show simulations of acquisition
after hippocampal stimulation with the M-S-S and S-P-H
models. Simulations with the M-S-S (Fig. 15a) and with
the S-P-H model (Fig. 15b) show that acquisition proceeded
faster in the treated group than in the control group

Figure 15a

M-S-S model: Delay conditioning after hippocampal
stimulation. HS: Hippocampal stimulation case. C:
control case. A : CS(A). X : Context. Left
Panels: NM response topography in 10 reinforced
trials. Upper-Right Panels: Net associative
values (VT) at the end of each trial, as a function
of trials. Lower-Right Panels: Associability
(ALPHA) at 350 msec, as a function of trials.
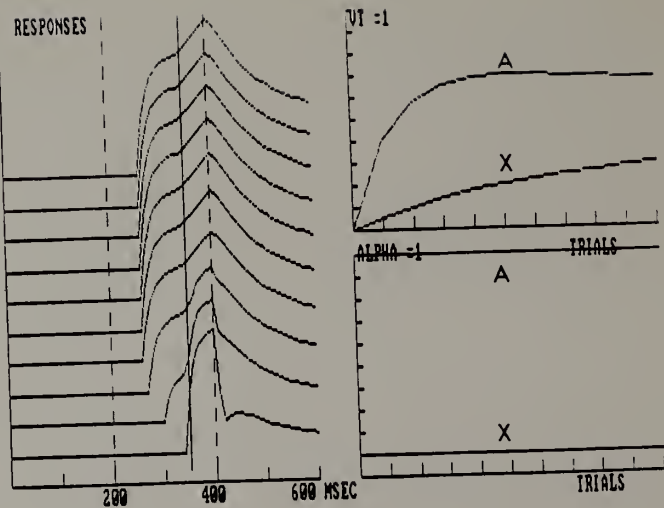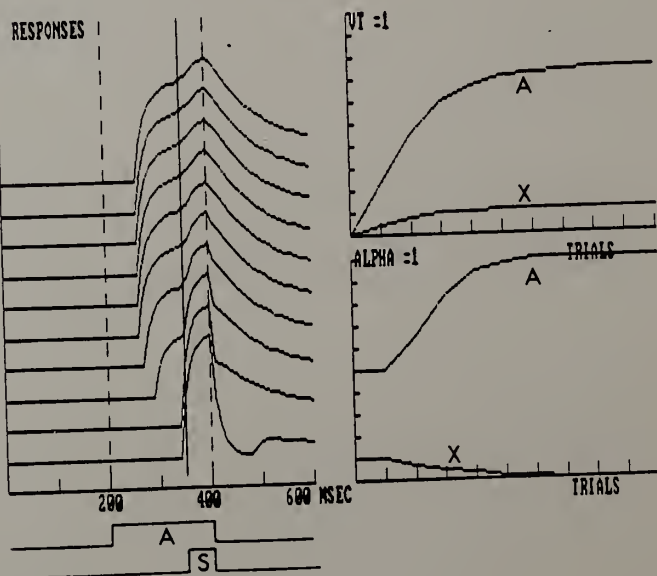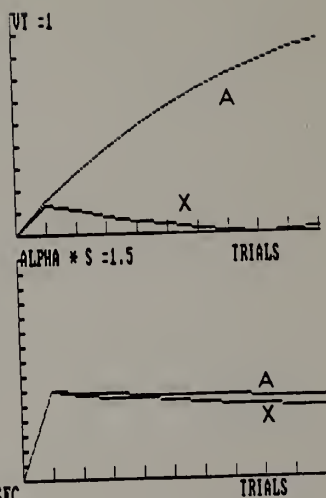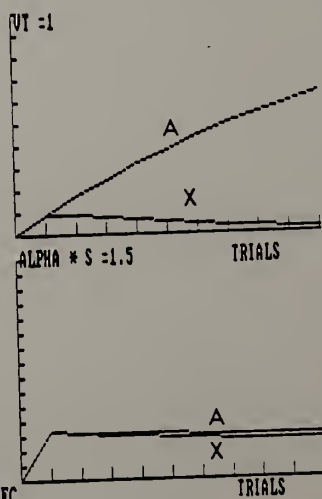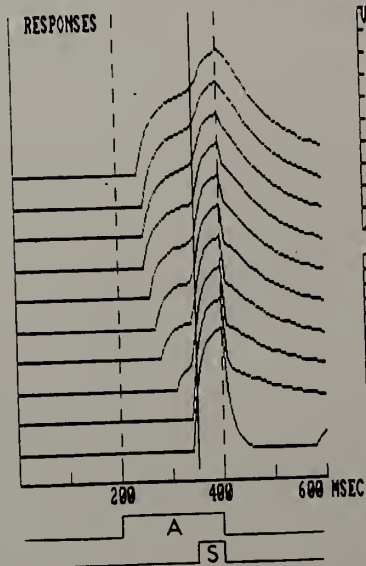
Figure 15b

S-P-H model: Delay conditioning after hippocampal
stimulation. HS: Hippocampal stimulation case. C:
control case. A : CS(A). X : Context. Left
Panels: NM response topography in 10 reinforced
trials. Upper-Right Panels: Net associative
values (VT) at the end of each trial, as a function
of trials. Lower-Right Panels: Associability
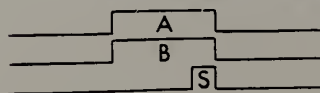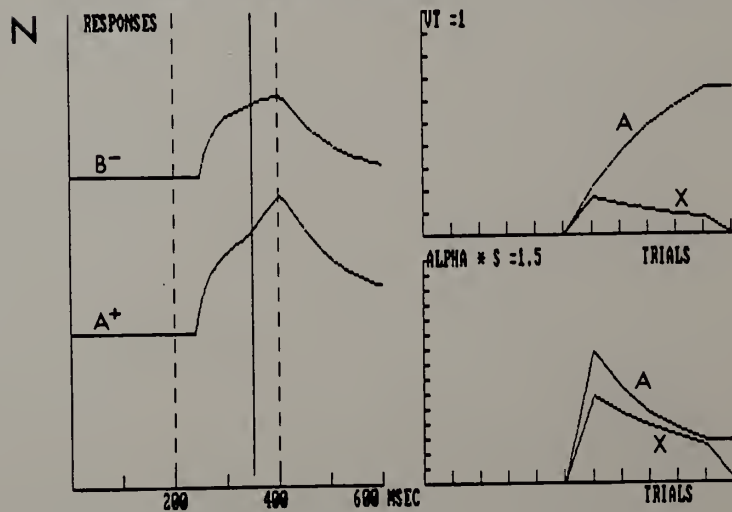(ALPHA) at 350 msec, as a function of trials.
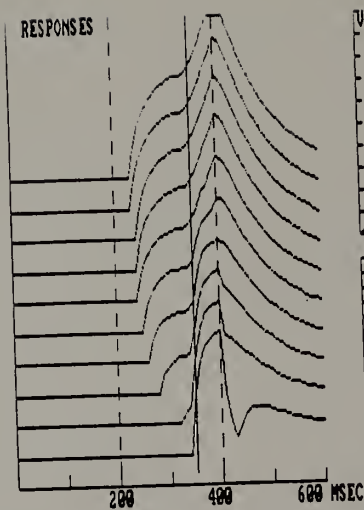
because of a larger associability. These results are in agreement with experimental data obtained by Berger (1984) and Prokasy et al. (1983).

Summary

Table 1 summarizes the results of the simulation experiments. The M-S-S model was able to describe the effects of HL on delay conditioning, trace conditioning with eye electrostimulation as US, conditioned inhibition, latent inhibition, blocking, and mutual overshadowing. The S-P-H model successfully described HL effects on trace conditioning with an air puff US, extinction, latent inhibition, blocking, discrimination reversal, and sensory preconditioning. The M-S-S model has problems simulating the behavior of HL animals under extinction, discrimination reversal, and sensory preconditioning. The S-P-H model has problems describing the behavior of HL animals in conditioned inhibition, and mutual overshadowing. The S-P-H model predicts that secondary reinforcement and serial compound conditioning are affected by HL, predictions that await experimental testing.

Both models rendered realistic simulations of the effect of HS on acquisition of classical conditioning.

Table 1. <u>Simulations of the M-S-S and S-P-H Models Compared with the Experimental Results of Classical Conditioning of the NM response.</u>

Paradigm	Observed HL Effect	Simulated HL Effect with model	
		M-S-S	S-P-H
Simultaneous Conditioning	?	0	+
Delay Conditioning	shorter latency	shorter latency	shorter latency
Trace Conditioning	shorter latency	normal latency *	shorter latency
Conditioned Inhibition	0	0	- *
Extinction	0	+ *	0
Latent Inhibition	-	- @	-
Blocking	-	-	-
Mutual Overshadowing	0	0	- *
Discrimination Reversal	-	0 *	-
	greater NM peak	normal NM peak*	greater NM peak
	greater CS area	normal CS area*	greater CS area
Sensory Preconditioning	-	0 *	-

	Neural Activity	Simulated neural activity with model	
		M-S-S	S-P-H
Acquisition	+	+	+

	Observed HS Effect	Simulated HS Effect with model	
		M-S-S	S-P-H
Acquisition	+ ˙	+	+

<u>Note.</u> HL = Hippocampal Lesion ; HS = Hippocampal Stimulation ; - = deficit; + = facilitation; 0 = no effect ; ? = no available data; * = the model fails to describe accurately the experimental result in the HL case. @ = the model fails to describe the experimental result in the normal case.

Also, realistic simulations of single unit recordings from
the hippocampus during acquisition of classical
conditioning were obtained with both models.

DISCUSSION

The present study introduces two models capable of
describing in real time classical conditioning of the
rabbit's NM response. The models are based on the M-S and
S-P-H models (Schmajuk and Moore, 1986), and they were
evaluated through computer simulations in various
classical conditioning paradigms.

Both models encompass higher-order conditioning,
yield topography of the rabbit's NM CR, predict the
effects of HL and HS on classical conditioning, and
describe hippocampal neuronal activity during
conditioning. These and other aspects of the models are
discussed in the following sections.

NM CR topography

The present study proposes performance rules that
convert net associative values into NM responses. With
these rules, both models simulate shorter CR latency in
the HL case than in the normal case for paradigms such as
delay conditioning or trace conditioning. Hoehler and
Thompson (1980), Port and Paterson (1984), and Solomon et
al. (in press, 1986) suggested that these decreased CR

latencies in HL animals are a consequence of an impairment
of HL animals for representing temporal relationships
between the CS and the US. Our results suggest that
decreased CR latencies are a consequence of attentional
changes in HL animals.

Although the performance rules allowed good
descriptions of NM topography, the rules present two
problems for the S-P-H model. The first problem is an
undesirable timing-intensity interaction. By Equation 21
the NM CR strength is proportional to the CS-US
associative value, and by Equation 20 the CR peak appears
at a time inversely proportional to the CS-US associative
value. By setting the threshold L1 in Equation 20,
performance rules can be applied to a given combination of
US intensity and ISI, predicting that the CR peak appears
at the time of the US presentation. However, once the
threshold L1 is set, increments in the US intensity
displace the predicted CR peak to an earlier time than
that of the US presentation. Therefore, a given threshold
L1 is valid only for a given combination of US intensity
and ISI. Since in the M-S-S model USs with different
intensities are treated as different events, this problem
only appears in the S-P-H model. Eventually, this problem
might be solved by independently storing two variables,
one related to the US intensity and the other to the US

timing.

The second problem with the performance rules is the inaccuracy of both models in defining the time of the CR peak for ISIs shorter than 200 msec. For ISIs longer than 200 msec, Equation 20 generates NM CRs with peaks approximately at the time when the US was presented. Because the trace decreases after 200 msec, both models predict that B decreases when ISI increases. Because longer ISIs imply smaller Bs, longer ISIs also imply a longer latency before

$\sum_t \sum_j B_j^{US}(t')$ by Equation 20 exceeds the treshold L1. Therefore the CR latency is longer and the CR peak appears approximately at the time of the US presentation. However, for ISIs shorter than 200 msec, Equation 20 generates NM CR peaks after the US presentation. This is so because the trace increases from 0 to 200 msec, and therefore B_j^{US} are directly proportional to ISI in the 0-200 msec temporal range. Because shorter ISIs imply smaller Bs, they imply a longer latency for $\sum_t \sum_j B_j^{US}(t)$ by Equation 20 to exceed treshold L1, and therefore CR begins later in the ISI and CR peak appears later than the time of the US presentation.

HL effects on the orienting response

In the P-H model associability has been related by
Kaye and Pearce (1984) to the orienting response towards a
CS, whereas associative values are related to both
attention towards a CS and to CR strength. Kaye and
Pearce (1984) report that the strength of the orienting
response (OR) during acquisition of classical conditioning
was inversely related to the predictive accuracy of the CS
toward which it is directed. They suggested that the
strength of the orienting response might be proportional
to $\propto$.

Assuming that $\propto$ determines the strength of the OR,
the S-P-H model predicts that animals with HL should have
stronger ORs than normals have. This is because $\propto$ for
the HL case is greater than $\propto$ for the normal case. All
simulations with the S-P-H model showed greater $\propto$ for the
HL than for the normal case. Supporting this prediction,
Powell and Buchanan (1980) report increased bradycardia
(an index of increased OR) over conditioning trials in HL
rabbits relative to controls.

Application of the models to other experimental paradigms

Although the present study was primarily concerned
with modelling hippocampal function in classical
conditioning of the rabbit's NM response, the models

obviously make contact with other conditioning paradigms in which relevant rabbit's NM data is sparse. This section contrasts HL effects on various protocols not considered previously, with computer simulations with the M-S-S and S-P-H models.

HL effects on differential conditioning.

Berthier and Moore (1980) investigated simple differential conditioning of the NMR to visual spatial CSs. HL rabbits did not differ from controls in responding to CS+, but they appeared to show fewer responses to CS-. However, it is not clear that CS-had actually become more inhibitory in HL animals than in controls because summation and retardation tests were not carried out. Micco and Schwartz (1972) report impairment in differential fear conditioning for HL rats. Although the effects of HL on differential conditioning have not been assessed in the NM preparation, they were nevertheless simulated using the M-S-S and the S-P-H models.

Differential conditioning was simulated by alternating two types of trials: reinforced trials consisted of a reinforced CS (A), and nonreinforced trials consisted of a nonreinforced CS (B). After 18 simulated trials for the normal case with both models, B acquires

inhibitory association. Simulations for the HL case with the M-S-S model show no difference from the normal case. Simulations for the HL case with the S-P-H model show that B had not acquired inhibitory associative value. Micco and Schwartz (1972) report impairment in differential fear conditioning for HL rats, in agreement with simulations obtained with the S-P-H model, but not with those obtained with the M-S-S model.

HL effects on conditional responding.

Orr, Holland, and Berger (1984), report impaired conditional responding in HL rats. Although the effects of HL on conditional responding have not been assessed in the NM preparation, they were nevertheless simulated using the M-S-S and the S-P-H model.

Conditional responding with the conditional cue preceding the CS cannot be simulated with the M-S-S model in its present form. With the M-S-S model, the CS acquires a higher V than the conditional cue because of its closer temporal relation to the US, and therefore it overshadows the cue. No conditional responding can occur because, as the conditional cue only accrues a small V, CR strength is determined mostly by the nominal CS.

The S-P-H model predicts impairments in conditional responding with the conditional cue preceding the CS as a

consequence of the absence of CS-CS associations.
Simulations consisted of 10 alternated presentations of
the conditional cue and the CS in the presence of the US,
and the CS alone. The CS acquires a smaller V than the
conditional cue because its S decreases by Equation 13 as
the CS is predicted by the conditional cue. Conditional
responding occurs because, as the CS only accrues a small
V, CR strength is determined mostly by the the conditional
cue. In the HL case responding is not possible because
conditional cue-CS associations are impaired, and
therefore the conditional cue does not predict the CS.
Since the conditional cue does not predict the CS, the CS
salience S does not decrease and the CS accrues a large V,
thereby eliciting a CR. These results agree with Ross, et
al.'s (1984) study reporting impaired conditional
responding in HL rats.

HL effects on serial-compound conditioning.

        Orr et al. (1984) report that acquisition of
associations between CS(A) and CR(B) were retarded in HL
rats in a conditional responding design where CS(A) was
followed by CS(B) and a US. Although the effects of HL on
serial-compound conditioning have not been assessed in the
NM preparation, they were nevertheless simulated using the
S-P-H models.

The S-P-H model predicts impairments in serial-compound conditioning as a consequence of the absence of CS-CS associations. In serial-compound conditioning, a CS(A) is paired with a US presented after a trace period following the termination of CS(A), and part of the trace period between CS(A) and the US is occupied by a CS(B). When CS(A) is paired with the US in the absence of CS(B) in a trace conditioning paradigm, CS(A) accrues less associative value than when CS(B) is interposed during the trace period. Interposing CS(B) during the trace period improves conditioning, presumably because of the formation of CS(A)-CS(B) and CS(B)-US associations that add associative value to the CS(A)-US trace conditioning.

In the context of the S-P-H model this result is explained by assuming that normal behavior is mediated through trace-conditioned CS(A)-CR(B) associations together with CS(A)-CS(B)-CR(B) second-order associations. HL behavior proceeds at a slower rate than normal because it is mediated only through CS(A)-CR(B) first-order associations.

Correspondence with neuroanatomical evidence.

This section examines possible functional correspondences between the M-S-S and S-P-H attentional-

associative models and the neurophysiology of several areas of the brain implicated in the conditioning of the rabbit's NM response.

Reflex circuit.

A tactile stimulus applied to the periocular region of the rabbit causes the eyeball to retract and the NM to sweep over the eyeball. This defensive reflex is mediated by a disynaptic circuit that comprises (Berthier & Moore, 1983): the tactile receptors in periocular areas and cornea, the opthalmic and maxillary branches of the VI (trigeminal) nerve, the sensory trigeminal nucleus, the accesory abducens nuclei, the VI nerve, and retractor bulbi muscle. The retractor bulbi muscles pull the eye into the socket and the nictitating membrane sweeps passively over the eyeball to protect it (Berthier, 1984; Moore & Desmond, 1981).

Electrical stimulation of the trigeminal nerve activates climbing fibers that project to the medial part of lobule VI and adjacent cerebellar areas (Miles and Weisendanger, 1975), a result that suggests that information about the US presentation is conveyed to the cerebellar cortex.

Cerebellar circuit.

Brain structures rostral to the red nucleus, including the neocortex are not essential for simple delay conditioning (Oakley and Russell, 1972). However, discrete lesions in the cerebellum can completly eliminate the CR without affecting the UR. For instance, Yeo, Hardiman, and Glickstein (1985a) report that removal of the hemispheric portion of lobule VI produces disruption of CRs. McCormick and Thompson (1984) found that destruction of the cerebellar dentate and interposed nuclei disrupts retention of ipsilateral CRs in the rabbit. Ipsilateral cerebellar lesions also prevent acquisition of the classically conditioned NM response (Lincoln, McCormick, and Thompson, 1982). Yeo, et al. (1985b) determined that the anterior interpositus nucleus is the critical region responsible for disruptive effects. Superior cerebellar peduncle lesions abolish the ipsilateral clasically conditioned NM response (McCormick, Guyer, and Thompson, 1982). Furthermore, multiunit activity increases at the dentate and interposed nuclei in the presence of the CR (McCormick, Lavond, and Thompson, 1983).

Lesions of deep cerebellar nuclei produce ipsilateral deficits in conditioning. Deep cerebellar nuclei send axons to the contralateral red nucleus via brachium conjunctivum, and lesions of the red nucleus disrupt

contralateral conditioned responding (Rosenfield and Moore, 1983). Desmond, Rosenfield, and Moore (1983) shows that neurons of the red nucleus project to the contralateral accesory abducens regions.

The above-mentioned evidence suggests that the flow of CS-US information originates in the hemispheric portion of cerebellar lobule VI, proceeds to the anterior interpositus nuclei, is relayed to the contralateral red nucleus, and finally reaches the contralateral accesory abducens nuclei. In this circuit, association of the CS (via mossy fibers from the lateral pontine nuclei) and the US (via climbing fibers from the inferior olive) would be mediated by plastic changes at the Purkinje cells of the cortical lobule HVI (Yeo, Hardiman, and Glickstein, 1985b).

Desmond and Moore (1985) report that a second system involving the dorsolateral pontine tegmentum also appears to be essential for the NM CR. Unilateral lesions of the dorsolateral pontine tegmentum eliminated ipsilateral but not contralateral CRs without affecting the URs (Desmond and Moore, 1982). Desmond and Moore (1985) suggested that this second system would be involved in learning to suppress eye-opening responses that compete with the NM CR by inhibiting the intermediate facial nucleus.

Information about CS-US associations might be

conveyed to the hippocampus through cerebellar-limbic system pathways. Heath (1973) report a monosynaptic pathway from the fastigial nucleus in the cerebellum to the septal region (nucleus of the diagonal band, nucleus accumbens) in the monkey. Harper and Heath (1973) report rostral connections of the fastigial nucleus in cat to hypothalamus, thalamus, nucleus accumbens, nucleus of the diagonal band, and dorsal anterior and medial septal nuclei. Heath and Harper (1974) report that, in both cats and monkeys, direct connections from the fastigial nucleus to temporal cortex, CA3 region in the hippocampus, dentate gyri, subicular regions, and amygdala. Although lesions of the fastigial nucleus do not produce NM CR impairment (Yeo, Hardiman, and Glickstein; 1985a), it might be involved in transmitting CR information from the cerebellum to the limbic system.

Neocortical circuit.

Although not essential for CS-US conditioning (Oakley and Russell, 1972), rostral areas of the brain may be necessary for the acquisition of CS-CS associations. Even when Port and Patterson (1984) report impairment of sensory preconditioning in rabbits with fimbrial lesions, some evidence suggests that CS-CS associations would be stored in the association cortex rather than in the

hippocampus. For instance, Segal (1974) failed to find changes in firing rates of hippocampal units in the rat after tone-light paired presentations, a result that would indicate that CS-CS associations are not stored in the hippocampus. Furthermore, Thompson and Kramer (1965) report that ablation of the association cortex in the cat precluded sensory preconditioning, a result supporting the idea that CS-CS associations are stored in the association areas of the neocortex.

Neocortical information reaches the hippocampus through multiple anatomical pathways. Papez (1927) suggested a closed loop involving hippocampus, mammilary bodies, anterior ventral thalamus, and cingulate gyrus. Output from the association cortex of the temporal and frontal lobes reach the hippocampus through the entorhinal area (Van Hoesen and Pandya, 1975). Reciprocally, outputs from the hippocampus reach the association cortex through the subiculum and posterior hippocampal gyrus (Irle and Markowitsch, 1982; Van Hoesen, 1980).

Hippocampal circuit.

The hippocampus has two major efferent projection systems, one cortical and the other subcortical. The cortical and subcortical projections would involve control of CS-CS and CS-US associations, respectively.

The hippocampus might exert its influence on neocortical storage of information through various pathways. One is the already mentioned Papez's circuit, interconnecting hippocampus with the cingulate cortex. The hippocampus is also connected to the association cortex through a closed circuit that involves the subicular complex, the thalamic nuclei, the association cortex, and the entorhinal cortex (Rosene and Van Hoesen, 1977; Van Hoesen, 1980).

Berger, et al. (1983) found that CA1 and CA3 pyramidal cells increased their frequency of firing over conditioning trials with a pattern that correlates with the amplitude-time course of the rabbit NM response. Both the M-S-S and the S-P-H models adequately describe this result.

In addition to CA1 and CA3 pyramidal cells, activity from other cells types have been recorded from the hippocampus during NM conditioning. For instance, Weisz, Clark, and Thompson (1984) found that granule cells in the dentate gyrus exhibited a stimulus-evoked theta firing when rabbits were trained with a CS followed by a US, but not when they were trained with CS and US unpaired presentations. According to Anchel and Lindsley (1975) hippocampal theta rhythm is correlated with the strength of the OR. It was indicated before that associability as

defined in the S-P-H model is correlated with the strength of the OR. Therefore, associability and theta activity would also be positively correlated. Consequently, activity of granule cells might be described by associability as defined in the framework of the S-P-H model.

Evidence has accumulated that some cells in the hippocampus would compare actual and predicted events, i.e., $(1 - \overset{.K}{\underset{L}{V}})$ in the M-S-S model or $\alpha = |\lambda^K - B^K|$ in the S-P-H model. For instance, Segal and Olds (1972) and Segal, Disterhoft, and Olds (1972) showed that cells in the CA1 and dentate regions increased in firing rates to a tone CS that preceded food US. When the tone CS was changed to precede an aversive US, the CA1 neurons continue to exhibit increased firing rate, but dentate cells decreased their firing rate. Specific cells in the dentate seem to be responsive to changes in the CS meaning. Consistent with these results, Deadwyler, West, and Robinson (1981) found that evoked potentials recorded from the dentate gyrus were associated to unexpected stimulus changes. Rank (1973) found cells in CA1 ("approach-consummate-mismatch" cells) that are most active when an expected US is not presented, and cells in CA3 ("approach-consummate" cells) that are most active before and during consummatory behaviors. Berger and

Thompson (1978a) noted that in the type of experiments
cited above, hippocampal cells first signalled a CS or a
place predicting a given CS, and afterwards signalled
their absence. This pattern of firing is well described
either by ($1 - \dot{V}_{\iota}^{K}$) or by $|\lambda - B^{K}|$. Both V_{ι}^{K} and B^{K}
increase with the temporal trace or the spatial proximity
of the rewarded CS. In the absence of the US, at the
point where the temporal trace reaches its maximum or the
CS approached, differences ($- V_{\iota}^{K}$) and
$|-B^{K}|$ reach a maximum value.

Some evidence suggests that the activity of some
hippocampal cells is correlated with the associability
value, as defined in both the M-S-S model and by Equation
12' in the S-P-H model. For example, Best and Best (1976)
report that tone presentation increased CA1 activity after
tone-US pairings in rats not preexposed to the tone (large
associability) but not in rats receiving tone pre-exposure
in a LI paradigm (small associability).

Berger and Thompson (1978b) recorded neuronal unit
activity from the medial septum during classic
conditioning of the rabbit NM. They found that medial
septal responses tend to decrease with repeated CS
presentations in both paired conditioning and unpaired
control groups. They suggested that neural activity in
medial septum represents an arousal signal that controls

hippocampal theta. This medial septal arousal signal is a precursor of the increased hippocampal unit activity during acquisition of classical conditioning. As in the case of granule cells, medial septal activity might be correlated with the value of associability as defined in the S-P-H model.

Berger and Thompson (1978a) proposed that the LTP effect would provide a possible mechanism for the sustained increased hippocampal unit activity during acquisition of classical conditioning. In both the M-S-S and S-P-H models the hippocampus computes and stores the value of the associability for every event. It is possible that LTP provides the mechanism for storing the associability values.

The hippocampus might exert its influence on cerebellar storage of information through several pathways. A hippocampal-retrospenial cortex projection via the subiculum reaches the ventral pons (Berger, Swanson, Milner, Lynch, and Thompson, 1980; Berger, Bassett, and Weikart, 1985; Semple-Rowland, Bassett, and Berger, 1981). Wyss and Sripanidkulchai (1984) reaffirmed the existence of cingulo-pontine projections described by Weisendanger and Weisendanger (1982). These cingulo-ventral pontine projections would modulate learning processes in the cerebellum, since the major output from

the ventral pontine nucleus are the mossy fibers to the
cerebellar cortex. Saint-Cyr and Woodward (1980) report
that Purkinje cells in the cerebellum were reliably
activated by fornix stimulation in the rat. Although the
pathways from the fornix to the cerebellum have not been
clarified, the input to the cebellum was found to
terminate on both mossy and climbing fibers. Responsive
cells were found in the hemispheric portion of lobule VI;
and lesions of this region produce disruption of CRs
(Glickstein et al., 1984).

Relationships to other hippocampal theories

As mentioned in the Introduction, both the M-S-S and
the S-P-H models belong to the attentional family of
hippocampal theories. Such group of theories propose that
after HL attentional control of environmental stimuli is
impaired. However, whereas most theories loosely defined
the meaning of attention and the effect of HL on it, both
models presented in this paper offer a precise
mathematical definition of attentional variables and of
the changes brought about in them after HL.

In the M-S-S model hippocampal function involves
learning to ignore irrelevant stimuli, a view shared with
a theory of the dorsal noradrenergic bundle (Mason and

Iversen, 1979). Mason and Iversen (1979) proposed a model in which noradrenaline is involved in learning to ignore irrelevant enviromental stimuli. This model can explain many effects of lesions of the dorsal noradrenergic bundle (DNB) and the pontine nucleus locus coeruleus (LC). As in the HL case, lesions of the DNB and the LC produce impairments in latent inhibition and blocking. Segal and Bloom (1976) found that LC stimulation augments inhibitory response in hippocampal unit activity to non-significant stimulus and augments excitatory response to a significant tone. If, as Segal and Bloom's (1976) findings suggest, some of the DNB functions are mediated through the hippocampus, then the M-S-S model might be used to describe the effect of DNB lesions.

In the S-P-H model the hippocampus participates in the comparison between actual and predicted events, a view shared with some earlier neural models of the hippocampus, e.g. Smythies (1966) and Gray (1982). According to Smythies (1966), the hippocampus compares environmental information coming from the entorhinal cortex with internal information coming from the septum. If two similar patterns of inputs are received, pyramidal neurons fire and the information is stored in the temporal cortex. Vinogradova (1975) argued that the CA3 region would be involved in evaluating the novelty of a signal coming from

the reticulo-septal circuit as compared to its counterpart in the cortical input. When novelty is detected an orienting response is elicited. According to Gray (1982) if actual and predicted events are the same, then behavior is maintained; if there is a mismatch the hippocampus inhibits the current behavior and attention is increased.

In the S-P-H model HL impairs the formation of CS-CS associations, an effect that might be equivalent to HL effects as described by other theories of hippocampal function. For example, Squire (1982) suggested that monkeys with combined hippocampal and amygdalar lesions were impaired in their ability to acquire new information about the world (declarative memory) but not in their ability to acquire new perceptual-motor skills (procedural memory). It is possible to equate declarative memory to CS-CS associations and procedural memory to CS-US associations. In the same vein, other authors proposed that the limbic-cortical regions of the brain would be involved in processes such as stimulus configuration (Mishkin and Petri, 1984), vertical associative memory (Wickelgren, 1979), or representational memory (Thomas and Spafford, 1984). Each of these processes may involve CS-CS associations. Striatal and cerebellar regions of the brain would be involved in processes such as habit formation (Mishkin and Petri, 1984), horizontal

associative memory (Wickelgren, 1979), or dispositional memory (Thomas and Spafford, 1984), each of which appear to involve CS-US associations.

Further improvements

Improved predictions of the effects of HL in both the M-S-S and S-P-H models might be obtained by assuming changes in computations different than those considered in this paper. For instance, in the M-S-S model it might be assumed that HL lesions preclude α either from decreasing, the assumption of the current model, or from increasing. Computer simulations indicate that such variation allows the M-S-S model to more accurately predict the experimental outcomes of a discrimination reversal paradigm in HL cases.

A more parsimonious description of HL effects with the S-P-H model is obtained by assuming that HL only impairs CS-CS associations and, as a consequence, that α is given by

$$\alpha = |\lambda^K - \sum_i \dot{v}_i^K| . \qquad [24]$$

Because α for HL animals computed with Equation 24 is larger than for normal animals given by Equation 12, use

of Equation 24 implies impairments in latent inhibition
and blocking. Computer simulations show that use of
Equation 24 allows the S-P-H model to improve its
predictions for HL effects on conditioned inhibition and
mutual overshadowing.

Conclusion

Both attentional-associative models considered in
this paper allow temporal simulation of learning processes
and their correlation with neural activity. The models
describe many classical conditioning paradigms in real-
time, including sensory preconditioning. Both models
yield CR topography of the rabbit NM response. In
addition to accurate descriptions of normal behavior, both
models correctly predict many effects of HL on classical
conditioning of the NM response.

BIBLIOGRAPHY

Anchel, H., & Lindsley, D.B. (1975). Differentiation of two reticulo-hypothalamic systems regulating hippocampal **Electroencephalography and Clinical Neurophysiology, 32,** 209-226.

Berger, T.W. (1984). Long-term potentiation of hippocampal synaptic transmission affects rate of behavioral learning. **Science, 224,** 627-630.

Berger, T.W., Alger, B., & Thompson, R.F. (1976). Neuronal substracte of classical conditioning in the hippocampus. **Science, 192,** 483-485.

Berger, T.W., Bassett, J.L., & Weikart, C. (1985). Hippocampal-cerebellar interactions during classical conditioning. The Twenty-sixth Annual Meeting of The Psychonomic Society. Boston, November 1985.

Berger, T.W., Clark, G.A., & Thompson, R.F. (1980). Learning-dependent neuronal responses recorded from limbic system brain structures during classical conditioning. **Physiological Psychology, 8,** 155-167.

Berger, T.W., & Orr, W.B. (1983). Hippocampectomy selectively disrupts discrimination reversal conditioning of the rabbit nictitating membrane response. **Behavioral Brain Research, 8,** 49-68.

Berger, T.W., Rinaldi, P.C., Weisz, D.J., & Thompson, R.F. (1983). Single-unit analysis of different hippocampal cell types during classical conditioning of rabbit nictitating membrane response. **Journal of Neurophysiology, 50,** 1197-1219.

Berger, T.W., Swanson, G.W., Milner, T.A., Lynch, G.S., & Thompson, R.F. (1980). Reciprocal anatomical connections between hippocampus and subiculum in the rabbit: Evidence for subicular innervation of regio superior. **Brain Research, 183,** 265-276.

Berger, T.W., & Thompson, R.F. (1978a). Neuronal plasticity in the limbic system during classical conditioning of the rabbit nictitating membrane response. I. The hippocampus. **Brain Research, 145,** 323-346.

Berger, T.W., & Thompson, R.F. (1978b). Neuronal plasticity in the limbic system during classical conditioning of the rabbit nictitating membrane response.

II. Septum and mammillary bodies. **Brain Research, 156,** 293-314.

Berger, T.W., & Thompson, R.F. (1982). Hippocampal cellular plasticity during extinction of classically conditioned nictitating membrane behavior. **Behavioural Brain Research, 4,** 63-76.

Berthier, N.E. (1984). The role of the extraocular muscles in the rabbit nictitating membrane response: A reexamination. **Behavioral Brain Research, 14,** 81-84.

Berthier, N. E., & Moore, J.W. (1983). The nictitating membrane response: An electrophysiological study of the Abducens nerve and nucleus and the Accesory Abducens nucleus in rabbit. **Brain Research, 258,** 201-210.

Best, M.R., & Best, P.J. (1976). The effects of state of conciousness and latent inhibition on hippocampal unit activity in the rat during conditioning. **Experimental Neurology, 51,** 564-573.

Buchanan, S.L., & Powell, D.A. (1980). Divergencies in Pavlovian conditioned heart rate and eyeblink responses produced by hippocampectomy in the rabbit (<u>Oryctolagus</u>

cuniculus). **Behavioral and Neural Biology, 30,** 20-38.

Clark, G.A., McCormick, D.A., Lavond, D.G., & Thompson, R.F. (1984). Effects of lesions of cerebellar nuclei on conditioned behavioral and hippocampal neuronal responses. **Brain Research, 291,** 125-136.

Deadwyler, S.A., West, M.O., & Robinson, J.H. (1981). Entorhinal and septal inputs differentially control sensory-evoked responses in the rat dentate gyrus. **Science, 211,** 1181-1183.

Desmond, J.E., & Moore, J.W. (1982). Brain stem elements essential for classically conditioned but not unconditioned nictitating membrane response. **Physiology and Behavior, 28,** 1092-1033.

Desmond, J.E., & Moore, J.W. (1985). Dorsolateral pontine tegmentum and the classically conditioned nictitating membrane response: Analysis of CR-related single-unit activity. Submitted.

Desmond, J.E., Rosenfield, M., & Moore, J.W. (1983). An HRP study of the brainstem afferents to the accesory abducens region and dorsolateral pons in rabbit:

Implications for the conditioned nictitating membrane response. **Brain Research Bulletin, 10,** 747-763.

Douglas, R., & Pribram, K.H. (1966). Learning and limbic lesions. **Neuropsychologia, 4,** 197-220.

Fox, S.E.,& Rank, J.B. Jr. (1975). Localization and anatomical identification of theta and complex spike cells in dorsal hippocampal formation in rats. **Experimental Neurology, 49,** 299-313.

Glickstein, M, Hardiman, M.J., & Yeo, C.H. (1984). Lesions of the cerebellar lobulus simplex abolish the classically conditioned nictitating membrane respons of the rabbit. **Journal of Physiology, 350,** 31P.

Gormezano, I. (1966). Classical conditioning. In J.B. Sidowski (Ed.), **Experimental Methods and Instrumentation in Psychology.** New York: McGraw-Hill.

Gormezano, I. (1972). Investigations of defense and reward conditioning in the rabbit. In A.H. Black and W.F. Prokasy (Eds.), **Classical Conditioning II: Theory and Research.** (pp 151-181). New York: Appleton-Century-Crofts.

Gormezano, I, Kehoe, E.J., & Marshall, B.S. (1983).
Twenty years of classical conditioning research with the
rabbit. **Progress in Psychobiology and Physiological
Psychology, 10**, 197- 275.

Grastyan, E., Lissak, K., Madaraz, I., & Donhoffer, H.
(1959). Hippocampal electrical activity during the
development of conditioned reflexes.
Electroencephalography and Clinical Neurophysiology, 11,
409-430.

Gray, J.A. (1982). Multiple book review of The
Neuropsychology of Anxiety: An inquiry into the functions
of the septo-hippocampal system. **The Behavioral and Brain
Sciences, 5**, 469-534.

Harper, J.W., & Heath, R.G. (1973). Anatomic connections
of the fastigial nucleus to the rostral forebrain in the
cat. **Experimental Neurology, 39**, 285-292.

Heath, R.G. (1973). Fastigial nucleus connections to the
septal region in the monkey and cat: A demonstration with
evoked potentials of a bilateral pathway. **Biological
Psychiatry, 6**, 193-196.

Heath, R.G., & Harper, J.W. (1974). Ascending projections of the cerebellar fastigial nucleus to the hippocampus, amygdala, and other temporal lobes sites: Evoked potential and histological studies in monkeys and cats. **Experimental Neurology, 45,** 268-287.

Hirano, T. (1984). Unit activity of the septo-hippocampal system in classical conditioning with rewarding brain stimulation. **Brain Research, 295,** 41-49.

Hoehler, F.K., & Thompson, R.F. (1980). Effect of the interstimulus (CS-UCS) interval on hippocampal unit activity during classical conditioning of the nictitating membrane response of the rabbit (Oryctolagus cuniculus). **Journal of Comparative and Physiological Psychology, 7,** 201-215.

Hull, C.L. (1943). **Principles of Behavior**. New York: Appleton-Century-Crofts.

Irle, E., & Markowitsch, H.J. (1982). Widespread cortical projections of the hippocampal formation in the cat. **Neuroscience, 7,** 2637-2647.

Kao, K.T., & Powell, D.A. (1983). Substantia nigra lesions and Pavlovian conditioning of eyeblink and heart rate response in the rabbit. **Society for Neurosciences Abstracts, 9,** 330.

Kaye, H., & Pearce, J.M. (1984). The strength of the orienting response during Pavlovian conditioning. **Journal of Experimental Psychology: Animal Behavior Processes, 10,** 90-109.

Kimble, D.P. (1968). Hippocampus and internal inhibition. **Psychological Bulletin, 70,** 285-295.

Lincoln, J.S., McCormick, D.A., & Thompson, R.F. (1982) Ipsilateral cerebellar lesions prevent learning of the classically conditioned nictitating membrane/eyelid response. **Brain Research, 242,** 190-193.

Lopes da Silva, F.H., Arnolds, D.E.A.T., & Neijt, H.C. (1984). A functional link between the limbic cortex and ventral striatum: Physiology of the subiculum accumbens pathway. **Experimental Brain Research, 55,** 205-214.

Mackintosh, N.J. (1975). A theory of attention : Variations in the associability of stimuli with

reinforcer. **Psychological Review**, **82**, 276-298.

Mason, S.T., & Iversen, S.D. (1979). Theories of the dorsal bundle extinction effect. **Brain Research Reviews**, **1**, 107-137.

McCormick, D.A., Guyer, P.E., & Thompson, R.F. (1982). Superior cerebellar peduncle lesions selectively abolish the ipsilateral classically conditioned nicitating membrane/ eyelid response of the rabbit. **Brain Research**, **244**, 347-350.

McCormick, D.A., Lavond, D.G., & Thompson, R.F. (1982). Concomitant classical conditioning of the rabbit nictitating membrane and eyelid responses: Correlations and implications. **Physiology and Behavior, 28,** 769-775.

McCormick, D.A., Lavond, D.G., & Thompson, R.F. (1983). Neuronal responses of the rabbir brainstem during performance of the classically conditioned nictitating membrane (NM)/eyelid response. **Brain Research, 271,** 73-88.

McCormick, D.A., & Thompson, R.F. (1984). Cerebellum: Essential involvement in the classically conditioned

eyelid response. **Science, 223,** 296-299.

Micco, D.J., & Schwartz, M. (1972). Effects of hippocampal lesions upon the development of Pavlovian internal inhibition in rats. **Journal of Comparative and Physiological Psychology, 76,** 371-377.

Miles, T.S., & Wiesendanger M. (1975). Climbing fibers inputs to cerebellar Purkinje cells from trigeminal cutaneous afferents and the SI face area of the cerebral cortex in the cat. **Journal of Physiology (London), 245,** 409-424.

Mishkin, M., & Petri., H.L. (1984). Memories and habits: Some implications for the analysis of learning and retention. In L.R. Squire and N. Butters (Eds.), **Neuropsychology of Memory.** New York: Guilford Press.

Moore, J.W. (1979). Brain processes and conditioning. In A. Dickinson and R.A. Boakes (Eds.), **Mechanisms of Learning and Behavior.** Hillsdale: Lawrence Erlbaum.

Moore, J.W., & Desmond, J.E. (1981). Latency of the nictitating membrane response to periocular electro-stimulation in unaesthetized rabbits. **Physiology and**

Behavior, 28, 1041-1046.

Moore, J.W., & Stickney, K.J. (1980). Formation of attentional-associative networks in real time: Role of the hippocampus and implications for conditioning. **Physiological Psychology, 8,** 207-217,

Moore, J.W., & Stickney, K.J. (1982). Goal tracking in attentional-associative networks: Spatial learning and the hippocampus. **Physiological Psychology, 10,** 202-208.

Moore, J.W., & Stickney, K.J. (1985). Antiassociations: Conditioned inhibition in attentional-associative networks. In R.R. Miller and N.E. Spear (Eds.), **Information processing in animals: Conditioned Inhibition.** Hillsdale: Lawrence Erlbaum.

Oakley, D.A. , & Russell, I.S. (1972). Neocortical lesions and Pavlovian conditioning. **Physiology and Behavior, 8,** 915-926.

O'Keefe, J., & Nadel, L. (1978). **The Hippocampus as a Cognitive Map.** New York: Oxford University Press.

Orr, W.B., & Berger, T.W. (1985). Hippocampectomy

disrupts the topography of conditioned nictitating membrane responses during reversal learning. **Journal of Comparative and Physiological Psychology, 99,** 35-45.

Papez, J.W. (1937). A proposed mechanism of emotion. **Archives of Neurology and Psychiatry, 38,** 725-744.

Pearce, J.M., & Hall, G. (1980). A model for Pavlovian learning: Variations in the effectiveness of conditioned but not of unconditioned stimuli. **Psychological Review, 87,** 532-552.

Pearce, J.M., Kaye, H., & Hall, G. (1982). Predictive accuracy and stimulus associability: Development of a model of Pavlovian learning. In M. Commons, R. Herrstein, & A.R. Wagner (Eds.), **Quantitative Analysis of Behavior** (Vol. 3). Cambridge, MA: Ballinger.

Port, R.L., Mikhail, A. A., & Paterson, M.M. (1985). Differential effects of hippocampectomy on classically conditioned rabbit nictitating membrane response related to interstimulus interval. **Behavioral Neuroscience, 99,** 200-208.

Port, R.L., & Paterson, M.M. (1984). Fimbrial lesions and

sensory preconditioning. **Behavioral Neuroscience, 98,**
584-589.

Powell, D.A., & Buchanan, S. (1980). Autonomic-somatic
relationships in the rabbit (Oryctolagus cuniculus):
Effects of hippocampal leions. **Physiological Psychology,**
8, 455-462.

Prokasy, W.F., Kesner, R.P., & Calder, L.D. (1983).
Posttrial electrical stimulation of the dorsal hippocampus
facilitates acquisition of the nictitating membrane
response. **Behavioral Neurosciences, 97,** 890-896.

Rank, J.B., Jr. (1973). Studies on single neurons in
dorsal hippocampal formation and septum in unrestrained
rats. **Experimental Neurology, 41,** 461-555.

Rescorla, R.A., & Wagner, A.R. (1972). A theory of
Pavlovian conditioning: Variations in the effectiveness
of reinforcement and non-reinforcement. In A. H. Black
and W.F. Prokasy (Eds.), **Classical Conditioning II:**
Theory and Research. New York: Appleton-Century-Crofts.

Rosenfield, M., & Moore, J.W. (1983). Red nucleus lesions
disrupt the classically conditioned nictitating membrane

response in rabbits. **Behavioral Brain Reseacrh, 10,** 393-398.

Rosene, D.L., & Van Hoesen, G.W. (1977). Hippocampal efferents reach widespread areas of the cerebral cortex and amygdala in the rhesus monkey. **Science, 198,** 315-317.

Ross, R.T., Orr, W.B., Holland, P.C., & Berger, T.W. (1984). Hippocampectomy disrupts acquisition and retention of learned conditional responding. **Behavioral Neurosciences, 98,** 211-225.

Saint-Cyr, J.A., & Woodward, D.J. (1980). A topographic analysis of limbic and somatic inputs to the cerebellar cortex in the rat. **Experimental Brain Research, 40,** 13-22.

Schmajuk, N.A. (1984a). Psychological theories of hippocampal function. **Physiological Psychology, 12,** 166-183.

Schmajuk, N.A. (1984b). A model for the effects of the hippocampal lesions on Pavlovian conditioning. **Abstracts of the 14th Annual Meeting of the Society for Neuroscience, 10,** 124.

Schmajuk, N.A., & Moore, J.W. (1985). Real-time attentional models for classical conditioning and the hippocampus. **Physiological Psychology** (In press).

Schmaltz, L.W., & Theios, J. (1972). Acquisition and extinction of a classically conditioned response in hippocampectomized rabbits **(Oryctolagus cuniculus).Journal of Comparative and Physiological Psychology, 79**, 328-333.

Schneiderman, N. (1966). Interstimulus interval function of the nicititating membrane response of the rabbbit under delay versus trace conditioning. **Journal of Comparative and Physiological Psychology, 62,** 397-402.

Schneiderman, N., & Gormezano, I. (1964). Conditioning of the nictitating membrane response of the rabbit as a function of the CS-US interval. **Journal of Comparative and Physiological Psychology, 57,** 188-195.

Segal, M. (1974). Convergence of sensory input on units in the hippocampal system of the rat. **Journal of Comparative and Physiological Psychology,** 87, 91-99.

Segal, M., & Bloom, F.E. (1976). The action of

norepinephrine in the rat hippocampus. IV. The effects of locus coeruleus stimulation on evoked hippocampal unit activity. **Brain Research, 107,** 513-525.

Segal, M., Disterhoft, J.F., & Olds, J. (1972). Hippocampal unit activity during classical aversive and appetitive conditioning. **Science, 173,** 680-690.

Segal, M., & Olds, J. (1972). Behavior of units in hippocampal circuit of the rat during learning. **Journal of Neurophysiology, 35,** 680-690.

Semple-Rowland, S.L., Bassett, J.L., & Berger, T.W. (1981). Subicular projections to retrospenial cortex in the rabbit. **Society for Neurosciences Abstracts, 7,** 886.

Smith, M.C. (1968). CS-US interval and US intensity in classical conditioning of the rabbit's nictitating membrane response. **Journal of Comparative and Physiological Psychology, 66,** 679-687.

Smythies, J.R. (1966). **Brain Mechanisms and Behavior.** New York: Academic Press.

Solomon, P.R. (1977). Role of the hippocampus in blocking

anD conditioned inhibition of rabbit's nictitating membrane response. **Journal of Comparative and Physiological Psychology, 91**, 407-417.

Solomon, P.R., & Moore, J.W. (1975). Latent inhibition and stimulus generalization of the classically conditioned nictitating membrane response in rabbits (**Orytolagus cuniculus**) following dorsal hippocampal ablation. **Journal of Comparative and Physiological Psychology, 89**, 1192-1203.

Solomon, P.R., Vander Schaaf, E.R., Thompson, R.F., & Weisz, D.J. (submitted). Hippocampus and trace conditioning of the rabbit's classically conditioned nictitating membrane response.

Squire, L.R. (1982). The neuropsychology of human memory. **Annual Review of Neuroscience, 5,** 241-273.

Swanson, L.W. (1978). The anatomical organization of septo-hippocampal projections. In K. Elliot and J. Whelan (Eds.) **Functions of the Septo-Hippocampal System.** New York: Elsevier.

Swanson, L.W., & Cowan, W.M. (1977). An autoradiographic

study of the organization of efferent connections of the hippocampal formation in the rat. **Journal of Comparative Neurology, 172,** 49-84.

Thomas, G.J., & Spafford, P.S. (1984). Deficits for representational memory induced by septal and cortical lesions (Singly and combined) in rats. **Behavioral Neuroscience, 98,** 394-404.

Thompson, R.F., & Kramer, R.F. (1965). Role of association cortex in sensory preconditioning. **Journal of Comparative and Physiological Psychology, 60,** 186-191.

Tolman, E.C. (1948). Cognitive maps in rats and men. **Psychological Review, 55,** 189-208.

Van Hoesen, G.W. (1980). The cortico-cortical projections of the posterior parahippocampal area in the rhesus monkey. **Anatomical Record, 196,** 195.

Van Hoesen, G.W., & Pandya, D.N. (1975). Some connections of the entorhinal and perirhinal (area 35) cortices on the rhesus monkey: I. Temporal lobe afferents. **Brain Research, 95,** 1-24.

Vinogradova, O.S. (1975). Functional organization of the limbic system in the process of registration of information: Facts and hypothesis. In R.L. Isaacson and K.H.Pribram (Eds.), **The Hippocampus**. New York: Plenum Press.

Wagner, A.R. (1979). Habituation and memory. In A. Dickinson and R.A. Boakes (Eds.), **Mechanisms of learning and Motivation**. Hillsdale, N.J.: Erlbaum.

Weisendanger, R., & Weisendanger, M. (1982). The corticopontine system in the rat. **Journal of Comparative Neurology, 208**, 227-238.

Weisz, D.J., Clark, G.A., & Thompson, R.F. (1984). Increased responsivity of dentate granule cells during nictitating membrane response conditioning in rabbit. **Behavioural Brain Research, 12**, 145-154.

Wickelgren, W.A. (1979). Chunking and consolidation: A theoretical synthesis of semantic networks, configuring in conditioning, S-R versus cognitive learnig, normal forgetting, the amnestic syndrome, and the hippocampal arousal system. **Psychological Review, 86**, 44-60.

Wyss, J.M., & Sripanidkulchai, K. (1984) The topography
of the mesencephalic and pontine projections from the
cingulate cortex. **Brain Research, 293**, 1-15.

Yeo, C.H., Hardiman, M.J., & Glickstein, M. (1985a).
Classical conditioning of the nictitating membrane
response of the rabbit: III. Connections of cerebellar
lobule HVI. **Experimental Brain Research, 60,** 114-126.

Yeo, C.H., Hardiman, M.J., & Glickstein, M. (1985b).
Classical conditioning of the nictitating membrane
response of the rabbit: I. Lesions of the cerebellar
nuclei. **Experimental Brain Research, 60,** 87-98.